Serafeim A.V., G. Kokosalakis, R. Deidda, I. Karathanasi and A. Langousis (2022), Probabilistic estimation of minimum night flow in water distribution networks: large-scale application to the city of Patras in western Greece. Stochastic Environmental Research and Risk Assessment, 36, 643–660. https://doi.org/10.1007/s00477-021-02042-9

Probabilistic Estimation of Minimum Night Flow in Water Distribution Networks: Large-scale Application to the City of Patras in Western Greece

By

Athanasios V. Serafeim[1], George Kokosalakis[1,2], Roberto Deidda[3], Irene Karathanasi[4], and Andreas Langousis[1]

[1]Department of Civil Engineering, University of Patras, Patras, Greece

[2]American College of Greece, Deree, School of Business and Economics
Department of Management and International Business, Athens, Greece

[3]Dipartimento di Ingegneria Civile, Ambientale ed Architettura
Università degli Studi di Cagliari, Cagliari, Italy

[4]Municipal Enterprise of Water Supply and Sewerage of the City of Patras, Patras, Greece

Submitted to:

SERRA

Submission dates:

Initial submission: March, 2021

Revised submission: May, 2021

Accepted: June, 2021

Correspondence: Andreas Langousis, Department of Civil Engineering, University of Patras, University Campus, 26504, Rio, Greece. Phone : +30(693)6898793, Fax: +30(210)4082055, e-mail: andlag@alum.mit.edu.

Abstract

We introduce two alternative probabilistic approaches for Minimum Night Flow (MNF) estimation in Water Distribution Networks (WDNs), which are particularly suited to minimize noise effects, allowing for a better representation of the low flows during night hours, as well as the overall condition of the network. The strong point of both approaches is that they allow for confidence interval estimation of the observed MNFs. The first approach is inspired by filtering theory, and proceeds by identifying a proper scale for temporal averaging to filter out noise effects in the obtained MNF estimates. The second approach is more intuitive, as it estimates MNF as the average flow of the most probable low-consumption states of the night flows. The efficiency of the developed methods is tested in a large-scale real world application, using flow-pressure data at 1-min temporal resolution for a 4-monthly winter period (i.e. November 2018 - February 2019) from the water distribution network of the City of Patras (i.e. the third largest city in Greece). Patras' WDN covers an area of approximately 27 km^2, consists of 700 km of pipeline serving approximately 213000 consumers, and includes 86 Pressure Management Areas (PMAs) equipped with automated local stations for pressure regulation. Although conceptually and methodologically different, the two probabilistic approaches lead to very similar results, substantiating the robustness of the obtained findings from two independent standpoints, making them suitable for engineering applications and beyond.

Keywords: Water Distribution Networks, Minimum Night Flow, Confidence Interval Estimation, Water losses

Highlights:

- Probabilistic Minimum Night Flow (MNF) estimation based on statistical metrics.
- Confidence interval estimates of observed MNFs for engineering applications.
- Robust representation of the low flows and the overall condition of the network.
- Large-scale application to the city of Patras, the third largest city in Greece.

1. Introduction

Leaks have a significant effect on the reduction of available water resources, but also on the management and operational costs of water distribution networks (WDNs; see e.g., Farley and Trow, 2005; Deng et al., 2013; Rehan et al., 2013, and Charalambous et al., 2014), as the lost water remains unbilled resulting in a reduction of the net revenue of the water supply and sewerage companies (see e.g. Lambert and Lalonde, 2005; Gomes et al., 2011; Mazzolani et al., 2016; Petroulias et al., 2016). Evidently, the increased operational expenses induced by water losses undermine WDNs' financial and environmental viability, with the latter being particularly critical given the ever-increasing demand for drinking water due to population growth, social and technological development (see e.g. Farley et al, 2001), as well as climate change effects and the uneven spatial and temporal distribution of rainfall (see e.g. IPCC, 2007; Bates et al., 2008; Ferguson et al., 2013; Langousis and Kaleris, 2014; Langousis et al., 2016; Mamalakis et al., 2017).

Aiming at a more complete formulation of the problem of water losses in WDNs, the International Water Association (IWA, see e.g. Lambert et al., 1999; Colombo et al., 2009) proposed the categorization of leakages into background losses and burst losses. Background losses are defined as the sum of small and possibly undetectable leaks, the localization and repair of which is deemed economically unprofitable, unless the water loss is gradually increased to the point where it is possible to detect and repair them in a cost effective setting. Burst losses are the real losses due to significant and extensive pipeline failures, which require immediate detection and repair, as they interfere with the operation of the network (see e.g. Lambert and Taylor, 2010, and Tsakiris and Charalambous, 2010). Since water losses caused by small and dispersed leaks are continuous, the corresponding volume of background losses is considerably larger and, therefore, economically and environmentally more impactful than that of burst losses.

The most common approach for estimation of background losses in WDNs is that of the minimum night flow (MNF, see e.g. Liemberger and Farley, 2004; Hunaidi and Brothers, 2007; Thornton et al., 2008; Tabesh et al., 2009; Cheung et al., 2010; Karadirek et al., 2012; Meseguer et. al., 2014). As human activity during late night and early morning hours is minimal (see e.g. Alkasseh et al., 2013 and AL-Washali et al., 2019), MNF estimates can be considered representative of the background losses in the network, as well as its overall condition (see e.g. AL-Washali et. al., 2020, and UN-Habitat et al., 2012). Under this setting, several studies have focused on applying MNF analysis to assess the level of background losses and condition of WDNs with significantly different characteristics.

For example, AL-Washali et. al. (2019) carried out a MNF analysis for an intermittent supply system in Zarqa (Jordan) using 5 days of flow data at 15-min resolution. Their results showed that the exact time of flow minima varied considerably between 00:00 am and 07:00 am, depending on the water levels in the consumers' tanks. Adlan et al. (2013) studied the frequency of night flow minima from 01:00 am to 05:00 am, using flow data at 15-min resolution for a 4-year period from 30 zones in Kinta Valley (Malaysia). They concluded that 84.2% of the MNF occurrences take place between 02:15 am and 04:15 am. Similar analyses were conducted by Verde et. al. (2014) and Muhammetoglu et. al. (2020). The first study performed extraction of night flow minima between 01:40 – 03:30 am using 1-min flow data from a small pressure management area (PMA) in Lenola, Rome (Italy), while the second study applied MNF analysis to flow data at 15-min resolution from Antalya (Turkey), in the time range between 00:00 – 05:00 am.

Bakogiannis and Tzamtzis (2014), Hamilton and McKenzie (2014) and Makaya (2017) restricted the MNF estimation range between 00:00 – 04:00 am. The same time range was used by Lee et al. (2005) for a small PMA in Korea (using 1-hour data), where land uses were divided into two distinct groups: business and residential. Their categorization was extended by Tabesh et. al. (2009) who noted that the maximum decrease in the night flow was observed from 03:00 am to 04:00 am, for residential users.

Estimation of MNF based on temporal averages has been increasingly gaining ground, as the corresponding estimates are more robust and less variable, reflecting the average condition of the network. For example, MacDonald and Yates (2005) used the average flow measured between 03:00 – 04:00 am in Halifax Regional Municipality (Canada) to approximate the MNF, while Covas et. al. (2008) applied two alternative approaches to extract MNF estimates in the time range between 02:00 am – 04:00 am, using 2-min data from 1 PMA in Lisbon, Portugal. The first approach consisted of matching the MNF estimate to the minimum flow value observed in the flow series at its original resolution (i.e. 2 min), whereas the second approach calculated the flow minimum after averaging the original series using a moving window of size equal to 10 min. The study concluded that the two approaches lead to similar results, but this should be primarily attributed to the small size of the averaging window applied.

In another, more recent study, Peters and Ben-Ephraim (2012) used flow data from Berbic (Guyana) at 15-min resolution for a period of 15 days, and calculated the MNF as the average of all flow measurements during the night hours from 02:00 – 04:00 am. The aforementioned operation resulted in much higher MNF estimates than those obtained when extracting the minima from the timeseries at their original resolution. In a similar context, Farah and Shahrour (2017) extracted MNF estimates during the 3-hour night period from 02:00 – 05:00 am, by applying a moving average window of size equal to 15 minutes to a 16-month long (January 2015 – April 2016) time series of flow measurements from the Scientific Campus of the University of Lille in France.

It follows from the discussion above that there are no rigorous specifications for the implementation of the MNF method and corresponding methodological assumptions, including the temporal resolution of the timeseries used to extract the flow minima, as well as the season of the year and the time-range of night hours to be included in the MNF analysis (see e.g. Butler and Memon, 2005; Hunaidi and Brothers 2007; Adlan et al., 2009; Brandt et al., 2017; Tabesh et al., 2009; Cheung et al., 2010; Loureiro et al., 2010; Alkasseh et al., 2013; Makaya, 2017). Notably, depending on the study/application, scanning and extraction of night flow minima from flow records may start (end) at different night (morning) hours, the seasonality of the consumption is usually ignored along with weekday effects, while the influence of the temporal resolution of the original time series on the extracted MNF estimates remains undetermined. Ignoring seasonality in the consumption time series may lead to biased MNF estimates (see e.g. WSAA, 2011), while not accounting for the temporal resolution of flow measurements results in unrealistically low MNF estimates, due to the significant variability of the high resolution signal; e.g. due to flow interruptions, radiation effects of pressure waves originating from network operations, equipment malfunctioning and/or aging effects, environmental conditions, suspended solid concentration, among many other factors (see e.g. Arregui et al., 2006; Quevedo et. al., 2012, and Hamilton and McKenzie, 2014). Currently, and to the best of our knowledge, there is no study that addresses background losses in a rigorous statistical context, to produce robust estimates based on average night flow conditions. The latter are also representative of the condition of the network.

To bridge this gap, the present work aims at developing two conceptually different probabilistic approaches for MNF estimation in WDNs, based on statistical metrics, followed by a large-scale application to the city of Patras, the third largest city in Greece, which consists of more than 700 km of pipeline partitioned into 86 pressure management areas (PMAs). The two approaches lead to very similar results, and are particularly suited to minimize noise effects, allowing for a better representation of the low flows during night hours, as well as the overall condition of the network. Their strong point is that they allow for confidence interval estimation of the observed MNFs, which makes them suitable for practical applications. The first approach is more elaborate, as it identifies a proper scale of temporal averaging to filter out noise effects in the estimation of MNF from the timeseries of night flow measurements during the low consumption period of the year (i.e. in the case of Greece and most Mediterranean countries, this period corresponds to the months from November to February, see e.g. Bisselink et. al, 2018, Serafeim, 2018, Tzanakakis et. al, 2020), without altering the signal of the daily consumption cycle (i.e. due to the increase in water demand during early morning hours). The second approach is more intuitive, as it estimates MNF as the average flow of the most probable states of the night flows during the low consumption period of the year.

The rest of the manuscript is organized as follows: Section 2 provides important details on the data used. The developed methodology for MNF estimation is outlined in Section 3, while important results from its application to the entire network of the city of Patras are presented and discussed in Section 4. Conclusions and future research directions are summarized in Section 5.

2. Data

In the analysis that follows, we use flow-pressure data at 1 min temporal resolution for the 4-month long consumption period from 01 November 2018 – 28 February 2019 (i.e. 119 days), which have been collected from the pressure regulation stations of the water distribution network (WDN) of the City of Patras in Western Greece. The network consists of more than 700 km of pipeline (mainly HDPE and PVC pipes) and 46 local pumping stations – pumping wells, covers an area of approximately 27 km^2, and serves approximately 213000 consumers (based on data from the Hellenic Statistical Authority and the Municipality of Patras), which correspond to more than 119000 authorized connections on the main network.

As shown in Figure 1 and indicated in Table 1, Patras' WDN is partitioned into 86 pressure management areas (PMAs), each one equipped with a local automated station for regulation of the inlet pressure; see Karathanasi and Papageorgakopoulos (2016). These stations are part of the "Integrated System for Pressure Management, Remote Operation and Leakage Control of the Water Distribution Network of the City of Patras", which is the largest smart water network (SWN) in Greece, with the Municipal Enterprise of Water Supply and Sewerage of the City of Patras (DEYAP) acting as the competent Authority for its operation and management.

The wider area of the City of Patras exhibits significant altitude differences, extending from the coast of the Gulf of Patras to Panachaiko Mountain. This significantly affects land uses, the spatial distribution of the population, as well as the water demand during different hours of the day. This constitutes an important feature of the large-scale application described in Section 4, as it allows for the developed methods and tools to be tested in a diverse set of PMA characteristics, including spatial coverage, as well as topographic and hydraulic constraints.

Flow-pressure data were acquired from DEYAP, for each of the 86 installed stations, and were quality assessed to detect and remove errors related to communication glitches. Zones exhibiting prolonged periods of system malfunctioning and/or pressure regulation issues (i.e. due to topographic constraints) were excluded from the analysis. Under this setting, 62 PMAs with less than 8% of missing values during the 4-month long period of low consumptions were identified to be used for MNF estimation. For this observational period, Table 2 summarizes the pressure set points during day (i.e. 06:00 am – 00:00 am) and night (i.e. 00:00 am – 6:00 am) hours, as well as the corresponding average flows. One sees that in some PMA's (e.g. 22, 25, 36, 84 among other, see Table 2) there is no difference between the pressure set points during day and night hours, as the upstream pressure is low enough, not requiring regulation.

3. Probabilistic approaches to MNF estimation

As noted in the Introduction, current approaches to MNF estimation are based on extraction of flow minima observed during night hours and ensemble averaging of the results from different days in the year. During the foregoing operation, seasonality of the consumption is usually ignored (in some cases the available record lengths do not exceed 1-2 months of flow measurements, irrespective of the seasonal pattern of the consumption), while the influence of the temporal resolution of the original time series on the extracted MNF estimates remains undetermined. While neglecting seasonality in the consumption may lead to overestimation of MNF estimates (see e.g. WSAA, 2011), ignoring the nominal resolution of the measurements may lead to unrealistically low MNF estimates, due to the significant variability of the high resolution signal. The latter may be induced by flow interruptions, radiation effects of pressure waves originating from network operations, equipment malfunctioning and/or aging effects, environmental conditions, suspended solid concentration, among many other factors; see Introduction.

In the next two subsections we introduce two alternative approaches for MNF estimation based on statistical metrics, which are particularly suited to minimize noise effects, allowing for a better representation of the low flows during night hours, as well as the overall condition of the network. The strong point of both approaches is that they allow for confidence interval estimation of observed MNFs. The first approach (hereafter referred to as Method 1) has been inspired by filtering theory, and proceeds by identifying a proper scale for temporal averaging of the night flows during the low consumption period of the year, to filter out noise effects in the obtained MNF estimates. The second approach (hereafter referred to as Method 2) is more intuitive, as it estimates MNF as the average flow of the most probable states of the night flows during the low consumption period of the year. The two approaches, which lead to similar MNF estimates, are first exemplified for PMA "Kentro" (the largest PMA of the Municipality of Patras), and then thoroughly applied to all zones of the network (see Section 4).

3.1. Probabilistic MNF estimation based on temporal averages (Method 1)

Statistical averaging (i.e. either simple or through kernel functions) has for a long time been used as an effective method to remove random fluctuations from data (see e.g. Wainstein and Zubakov,1970). In this context, we seek for a proper scale/duration D (see below) to average the original time series and estimate MNF as the ensemble mean, $\bar{Q}_{min,D}$, of the minimum average flows $Q^{(j)}_{min,D}$ estimated during the night hours in different days j of the low consumption period of the year (for the City of Patras, and most Mediterranean regions, this period extends from the month of November to February):

$$\bar{Q}_{min,D} = \frac{1}{n}\sum_{j=1}^{n} Q^{(j)}_{min,D} = \frac{1}{n}\sum_{j=1}^{n}\left(\min_{u}\{Q^{(j)}_{D}(u)\}\right) \quad (1)$$

where $u \in [t_1 + D/2,\ t_2 - D/2]$, $[t_1, t_2]$ is the night hour range (in our case from 00:00 am – 6:00 am, i.e. $\Delta T = t_2 - t_1 = 6$ hours), D is a properly selected averaging duration (see below), n is the number of days in the low consumption period, and:

$$Q^{(j)}_{D}(u) = \frac{1}{D}\int_{u-D/2}^{u+D/2} Q^{(j)}(t)\, dt \quad (2)$$

where $Q^{(j)}(t)$ is the flow time series at its nominal resolution in day j.

Figure 2 shows average flows $Q^{(j)}_{D}(u)$ for 27 December 2018, calculated using equation (2) for various window sizes D in the range from 1 min to 3 hours for PMA "Kentro", in the time frame $u \in [00{:}00 + D/2,\ 06{:}00\ \text{am} - D/2]$. One sees the gradual reduction in the demand from 00:00 am - 04:00 am (late night), followed by a 1-hour period (i.e. 04:00 am - 05:00 am) of approximate stabilization to a state of low flows, and a subsequent increase of the consumption due to the onset of human activity in morning hours. Figure 3 summarizes the corresponding minima $Q^{(j)}_{min,D} = \min_{u}\{Q^{(j)}_{D}(u)\}$ of the time series in Figure 2, as a function of the averaging duration D. One sees that the observed minima increase fast with increasing size of the averaging window D up to 60 min, with the minimum rate of increase being observed somewhere between 60 and 120 min. For values of D larger than 120 minutes, the observed minima increase again fast with increasing D due to early morning effects (as illustrated in Figure 2).

A behavior similar to Figure 3 is observed also in Figure 4, which shows the ensemble mean $\bar{Q}_{min,D}$ of equation (1) (i.e. obtained by averaging $Q^{(j)}_{min,D}$ over all days $j = 1, 2, \ldots, n$ in the 4-monthy low consumption period) for PMA "Kentro" as a function of D. One clearly sees the formation of two distinct regions: Region I in Figure 4 reflects primarily the effects of noise reduction due to statistical averaging, while Region II (same Figure) illustrates the effects of the increase in the consumption during the early morning hours.

Under this setting, one concludes that the size of the averaging window D used for MNF estimation based on equation (1) should be large enough to smooth out random fluctuations (i.e. noise) in the high resolution signal and, also, should not exceed an upper limit above which increase of consumption positively biases the MNF estimates. To do so in a rigorous statistical setting, we estimate a proper size for the averaging window D^* by ensemble averaging the correlation length estimates d_j (i.e. the lag at which the autocorrelation function equals zero) of the flow time series during the night hours of each day j in the low consumption period:

$$D^* = \frac{1}{n}\sum_{j=1}^{n} d_j \tag{3}$$

where $d_j := \{d: \rho_j(d) = 0\}$, and $\rho_j(d)$ is the autocorrelation function of the flow time series $\{Q^{(j)}(t), t \in [t_1, t_2]\}$ in day $j = 1, 2, \ldots, n$.

For the aforementioned procedure to result in reliable D^* estimates, the correlation lengths d_j should be normally distributed around their mean, indicating the presence of random fluctuations. In this context, for PMA "Kentro", Figure 5 shows the empirical cumulative distribution function (eCDF, circles) of d_j estimates, obtained as the correlation lengths of the flow time series during the night hours of different days j in the 4-monthy low consumption period. One sees that the obtained estimates are in good approximation normally distributed (p-value of 40.9 % according to Lilliefors's test for unknown mean and variance; see Lilliefors, 1967 and Dallal and Wilkinson, 1986) with mean value $m_d = D^* = 119.3 \approx 120$ min (see also equation (3)) and standard deviation $\sigma_d = 5.82$ min (i.e. $d_j \sim N(D^*, \sigma_d^2)$). This indicates that the observed deviations of the d_j estimates from their ensemble mean can be attributed to sampling variability.

Similar to Figure 5, for PMA "Kentro" and for size of the averaging window $m_d = D^* =$ 120 min (see above), Figure 6 shows the eCDF (circles) of the estimates $Q^{(j)}_{min,D*}$ of the minimum average flow in different days $j = 1, 2, \ldots, n$ of the 4-monthy low consumption period. One sees that the obtained estimates are in good approximation normally distributed (Lilliefors's test p-value of 79.9 %), with mean value $\bar{Q}_{min,D*} = 69.40$ l/s (see also equation (1)) and standard deviation $\sigma_Q = 4.37$ l/s (i.e. $Q^{(j)}_{min,D*} \sim \mathrm{N}(\bar{Q}_{min,D*}, \sigma_Q^2)$). The latter finding is a direct consequence of the central limit theorem (CLT, see e.g. Parzen, 1960; Fisz, 1963; Feller, 1968, Benjamin and Cornell, 1970, and Papoulis, 1990), as $Q^{(j)}_{min,D*}$ estimates are obtained as statistical averages of $r = D^*/\tau$ flow observations, where τ is the nominal resolution of the time series (i.e. in our case $\tau = 1$ min and $r = D^*/\tau = 120$). Since $Q^{(j)}_{min,D*}$ are in good approximation normally distributed, their mean value $\bar{Q}_{min,D*}$ can also be considered in good approximation normally distributed, allowing for both point and confidence interval estimation of MNF. More precisely, the point estimate of the MNF in PMA "Kentro" is obtained as:

$$\widehat{\mathrm{MNF}} := \bar{Q}_{min,D*} \quad (4)$$

while the (1-α)·100 percent two sided confidence interval can be obtained from the probability statement (see e.g. Benjamin and Cornell, 1970):

$$P\left[- t_{\alpha/2,\, n\text{-}1} < \frac{\widehat{\mathrm{MNF}} - \mathrm{MNF}}{\sigma_Q/\sqrt{n}} \leq + t_{\alpha/2,\, n\text{-}1}\right] = P\left[- t_{\alpha/2,\, n\text{-}1} < \frac{\bar{Q}_{min,D*} - \mathrm{MNF}}{\sigma_Q/\sqrt{n}} \leq + t_{\alpha/2,\, n\text{-}1}\right] = 1- \alpha \quad (5)$$

where n is the number of days in the low consumption period, and $t_{\alpha/2}$ is the value exceeded with probability $\alpha/2$ by a random variable that follows a Student's t - distribution with n-1 degrees of freedom. Thus:

$$P\left[\bar{Q}_{min,D*} - \frac{\sigma_Q}{\sqrt{n}}\, t_{\alpha/2,\, n-1} < \text{MNF} \le \bar{Q}_{min,D*} + \frac{\sigma_Q}{\sqrt{n}}\, t_{\alpha/2,\, n-1}\right] = 1 - \alpha \tag{6}$$

For PMA "Kentro", the point estimate of MNF is $\widehat{\text{MNF}} = \bar{Q}_{min,D*} = 69.40$ l/s, while the 95% two sided confidence interval is [68.61, 70.19] l/s.

3.2. Probabilistic MNF estimation based on the concept of most probable states (Method 2)

Figure 7.a illustrates the 1-min resolution timeseries of flow measurements in PMA "Kentro" on 27 December 2018 within the time frame from 00:00 am to 06:00 am (see also Figure 2), and Figure 7.b shows their corresponding empirical probability density function (ePDF). One clearly sees that the empirical distribution is positively skewed (i.e. skewed to the right), revealing the prevalence of low flows during night hours, and further characterized by three distinct Regions: Region A (see Figures 7.a and 7.b) contains flow values observed between 00:00 am - 01:05 am (late night), Region B is composed by flow values observed between 01:05 am – 03:00 am (late night) and 05:40 am – 06:00 am (early morning), and Region C includes the low flows during the night hours from 03:00 am – 05:40 am. An important observation is that the lowest modal value (i.e. the lowest most frequent value) of the distribution is observed in Region C, and can be considered representative of the MNF, as the latter is linked to the most probable low-consumption state of the PMA during night hours, when human activity is minimal. In this context, in what follows we estimate MNF as the ensemble mean, $\bar{Q}_{lmod}$, of the lowest modal values $Q_{lmod}^{(j)}$ observed during the night hours of different days j in the low consumption period:

$$\bar{Q}_{lmod} = \frac{1}{n}\sum_{j=1}^{n} Q_{lmod}^{(j)} \tag{7}$$

where $Q_{lmod}^{(j)}$ denotes the lowest modal value (i.e. the lowest most frequent value) of the empirical PDF of observed flows within the night hour range (in our case from 00:00 am – 6:00 am) of day j (j = 1, 2, …, n), and n is the number of days in the 4-monthy low consumption period.

For the aforementioned procedure to result in reliable MNF estimates, the lowest modal values $Q_{lmod}^{(j)}$ should be normally distributed around their mean, indicating the presence of random fluctuations. In this context, for PMA "Kentro", Figure 8 shows the empirical cumulative distribution function (eCDF) of the lowest modal values $Q_{lmod}^{(j)}$, estimated from the flow time series during the night hours in different days j of the 4-monthy low consumption period. One sees that the obtained estimates are in good approximation normally distributed (Lilliefors's test p-value of 5.7 %), with mean value $\bar{Q}_{lmod}$ = 69.85 l/s (see also equation (7)) and standard deviation σ_{Qlm} = 3.91 l/s (i.e. $Q_{lmod}^{(j)} \sim \mathrm{N}(\bar{Q}_{lmod}, (\sigma_{Qlm})^2)$).

Since $Q_{lmod}^{(j)}$ are in good approximation normally distributed, their mean value $\bar{Q}_{lmod}$ can also be considered in good approximation normally distributed, allowing for both point and confidence interval estimation of MNF. More precisely, the point estimate of the MNF in PMA "Kentro" is obtained as:

$$\widehat{\mathrm{MNF}} := \bar{Q}_{lmod} \tag{8}$$

while the (1-α)·100 percent two sided confidence interval can be obtained from the probability statement (see e.g. Benjamin and Cornell, 1970):

$$P\left[-t_{\alpha/2,\,n\text{-}1} < \frac{\widehat{\mathrm{MNF}} - \mathrm{MNF}}{\sigma_{Qlm}/\sqrt{n}} \le +t_{\alpha/2,\,n\text{-}1}\right] = P\left[-t_{\alpha/2,\,n\text{-}1} < \frac{\bar{Q}_{lmod} - \mathrm{MNF}}{\sigma_{Qlm}/\sqrt{n}} \le +t_{\alpha/2,\,n\text{-}1}\right] = 1 - \alpha \quad (9)$$

where n is the number of days in the low consumption period, and $t_{\alpha/2}$ is the value exceeded with probability $\alpha/2$ by a random variable that follows a Student's t - distribution with n-1 degrees of freedom. Thus:

$$P\left[\bar{Q}_{lmod} - \frac{\sigma_{Qlm}}{\sqrt{n}}\, t_{\alpha/2,\,n\text{-}1} < \mathrm{MNF} \le \bar{Q}_{lmod} + \frac{\sigma_{Qlm}}{\sqrt{n}}\, t_{\alpha/2,\,n\text{-}1}\right] = 1 - \alpha \quad (10)$$

For PMA "Kentro", the point estimate of MNF is $\widehat{\mathrm{MNF}} = \bar{Q}_{lmod} = 69.85$ l/s, while the 95% two sided confidence interval is [69.15, 70.55] l/s.

An important note to be made here, is that while the MNF estimation methods outlined in this and the previous sub-sections are conceptually and methodologically different, they lead to very similar results, substantiating the robustness of the obtained findings from two independent standpoints.

In the next section, we further investigate the robustness of the developed approaches for MNF estimation via a thorough application to 62 PMAs of Patras WDN and, also, intuitively explain observed deviations from normality found in 6 PMAs, based on conducted flow-pressure tests.

4. Results and discussion

Table 3 summarizes the point estimates and 95% confidence interval estimates of the average MNF calculated for the 62 PMAs of Patras WDN, using Methods 1 and 2, along with the standard deviations and corresponding Lilliefors's test p-values of the individual MNF estimates obtained for each day of the 4-monthy low consumption period analyzed. Further, for Method 1, Table 4 summarizes the size of the averaging window $D^* = m_d$ used to apply equation (1) to each analyzed PMA, along with the standard deviation and corresponding Lilliefors's test *p*-value of the individual d_j estimates calculated for each day *j* in the low consumption period.

One sees that with the exception of 6 PMAs (i.e. Bounteni_4 (26), Bounteni_5 (27), Elekistra_1_2_3 (36), Elekistra_4 (37), Elos (38) and Karya_5 (49); see discussion on flow - pressure tests below), the daily MNF estimates obtained by both methods (see Table 3) are in good approximation normally distributed, with Lilliefors's test *p*-values that exceed 5%. In addition, as illustrated in Figure 9, the obtained point estimates of the average MNF lie along the 1:1 - line, indicating that although conceptually and methodologically different, the two methods converge to very similar results, with a negligible overestimation by Method 2 (see also Table 3). The same holds also for the 95% confidence interval estimates of the average MNF, as a direct consequence of equations (6) and (10).

To further investigate the observed deviations from normality and their possible linkage to background losses, we conducted flow-pressure tests in 43 out of the 62 PMAs studied, including the 6 PMAs mentioned above (i.e. Bounteni_4 (26), Bounteni_5 (27), Elekistra_1_2_3 (36), Elekistra_4 (37), Elos (38) and Karya_5 (49)). The flow pressure tests were conducted by applying three different night pressure set points for a minimum of 5 nights each. During selection of the corresponding pressure ranges, particular care was taken to avoid possible water supply disruptions at critical points of the network induced by low pressure levels, as well as possible pipeline failures induced by high pressures. Table 5 summarizes the pressure ranges applied to each PMA, along with the corresponding periods of their application, and Figure 10 illustrates MNF estimates for eight PMAs obtained using Method 1, as a function of the applied night pressure.

The first two PMAs in Figure 10 (i.e. 4 (Ano_syxaina_1, Figure 10.a), and 64 (Pagona_H, Figure 10.b)) have been selected as representative of PMAs with daily MNF estimates that are in good approximation normally distributed, with Lilliefors's test *p*-values of 52.6% (35.4%) and 51.2% (72.9%) according to Method 1 (2), respectively; see Table 3. The remaining six PMAs (i.e. 26 (Bounteni_4, Figure 10.c), 27 (Bounteni_5; Figure 10.d), 36 (Elekistra_1_2_3, Figure 10.e), 37 (Elekistra_4, Figure 10.f), 38 (Elos, Figure 10.g) and 49 (Karya_5, Figure 10.h); see bold values in Table 3), are those identified during the implementation of Method 1 as those exhibiting Lilliefors's test *p*-values well below 5%, indicating significant deviations from the normality assumption.

Despite the high variability of the obtained MNF estimates observed in all sub-figures, it becomes apparent that for PMAs where the normality assumption is substantiated statistically (e.g. PMAs 4 and 64, see Figures 10.a and 10.b), the MNF increases with increasing inlet pressure signifying that the component of background losses in the MNF estimates is important, as outlined by Torricelli's law and indicated by the substantial positive slope of the corresponding linear least squares fits. For those PMAs that the normality assumption is not statistically significant (i.e. Lilliefors's test *p*-values well below 5%; see Figures 10.c - 10.h), the dependence of the obtained MNFs on pressure is rather marginal, as indicated by the small positive or negative slopes of the corresponding least squares fits. Note that negative slopes cannot be justified physically, and should be attributed to the statistical variability of the night consumption that dominates the MNF estimates.

Along these lines, and at least for Patras WDN, cases when the MNF estimates deviate significantly from the normal shape can be seen as a strong indication that background losses constitute only a small portion of the estimated night flow minima, with the statistical variability of the latter being primarily determined by the fresh water consumption during night hours.

5. Conclusions

While quantification of background losses in Water Distribution Networks (WDNs) and assessment of their overall condition is usually based on minimum night flow (MNF) estimates, no rigorous statistical methodology currently exists that produces robust estimates based on average night flow conditions. In this context, the present study aimed at developing two alternative probabilistic approaches for MNF estimation in WDNs, based on statistical metrics, followed by a large-scale application to the city of Patras, the third largest city in Greece.

The first approach, inspired by filtering theory, is based on the identification of a proper scale for temporal averaging of night flows during the low consumption period of the year, to filter out noise effects in the obtained MNF estimates. The second approach is more intuitive, estimating MNF as the average flow of the most probable states of the night flows during the low consumption period of the year. Although conceptually and methodologically different, the two approaches led to very similar results, substantiating the robustness of the obtained estimates from two independent standpoints.

An additional important finding, is that in almost all cases (with the exception of 6 pressure management areas (PMAs), common to both methods, see below) and independent of the network specific characteristics (e.g. length of the pipeline grid, land usage, altitude differences etc.), the MNF estimates obtained by applying both methods to 62 PMAs of the City of Patras were in good approximation normally distributed (i.e. Lilliefors's test *p*-values above 5%), allowing for both point and confidence interval estimation of the average MNF. For the 6 PMAs where the MNF estimates deviated significantly from the normal shape, the conducted flow pressure tests showed that the dependence of the obtained MNFs on the inlet pressure was marginal, indicating that background losses constitute only a small portion of the estimated night flow minima, with the statistical variability of the latter being primarily determined by the consumption during night hours.

Since both developed methods lead to very similar MNF estimates independent of PMA characteristics, and given that Method 1 is more tedious to apply than Method 2, we believe that the latter method can serve as a useful tool for engineering applications, allowing agencies and competent authorities to advance their current practices on flow-pressure management and quantification of background losses based on a fully probabilistic framework. Future research should focus on advancing the developed framework to allow parameterization of MNF estimates as a function of the inlet pressure, and PMA specific characteristics (i.e. pipe diameters, length of the pipeline grid, intensity of the topography etc.).

Acknowledgments

The research project was supported by the Hellenic Foundation for Research and Innovation (H.F.R.I.) under the “1st Call for H.F.R.I. Research Projects to support Faculty Members & Researchers and the procurement of high-cost research equipment grant” (Project Number: 1162). The Authors would like to acknowledge the useful comments and suggestions received by Dr. G. Pegram and one anonymous Reviewer, which significantly improved the presented work.

Declaration of Interests

The Authors declare that they have no known competing financial interests or personal relationships that could have appeared to influence the work reported in this paper.

References

Adlan, M.N., H.A. Aziz, N.M. Razib and A.B.M. Hanif (2009) The effects of pressure reduction on Non-Revenue Water in water reticulation system, *International Conference on Water Conservation in Arid Regions*, Kingabdul Aziz University, Jeddah, Saudi Arabia.

Adlan, M.N., J.M.A. Alkasseh, H.I. Abustan and A.B.M. Hanif (2013) Identifying the appropriate time band to determine the minimum night flow: a case study in Kinta Valley, Malaysia, *Water Supply*, **13**(2), p.p. 328-336, DOI: 10.2166/ws.2013.026.

Alkasseh, J.M.A., M.N. Adlan, I. Abustan, H.A. Aziz and A.B.M. Hanif (2013) Applying Minimum Night Flow to Estimate Water Loss Using Statistical Modeling: A Case Study in Kinta Valley, Malaysia, *Water Resources Management*, **27**(5), p.p. 1439-1455, DOI: 10.1007/s11269-012-0247-2.

AL-Washali, T., S. Sharma, F. AL-Nozaily, M. Haidera and M. Kennedy (2019) Modelling the Leakage Rate and Reduction Using Minimum Night Flow Analysis in an Intermittent Supply System, *Water*, **11**(1) 48, DOI: 10.3390/w11010048.

AL-Washali, T., S. Sharma, R. Lupoja, F. AL-Nozaily, M. Haidera and M. Kennedy (2020) Assessment of water losses in distribution networks: Methods, applications, uncertainties, and implications in intermittent supply, *Resources, Conservation and Recycling*, **152**, DOI: 10.1016/j.resconrec.2019.104515.

Arregui, F.J., E. Cabrera, R. Cobacho and J. García-Serra (2006) Reducing Apparent Losses Caused By Meters Inaccuracies, *Water Practice and Technology*, **1**(4), DOI: 10.2166/wpt.2006.093.

Bakogiannis, A. and A. Tzamtzis (2014) Modeling of district metered areas with relatively high leakage rate. The case study of Kalipoli's DMA, *CUNY Academic Works*, https://academicworks.cuny.edu/cc_conf_hic/384.

Bates, B.C., Z.W. Kundzewicz, S. Wu. and J.P. Palutikof, Eds. (2008) Climate Change and Water. Technical Paper of the Intergovernmental Panel on Climate Change, *IPCC Secretariat*, Geneva, p.p. 210, ISBN: 978-92-9169-123-4.

Benjamin, J. R., and C. A. Cornell (1970) Probability, Statistics, and Decision for Civil Engineers, *McGraw-Hill*.

Bisselink, B., J. Bernhard, E. Gelati, M. Adamovic, S. Guenther, L. Mentaschi and A. De Roo (2018) Impact of a changing climate, land use, and water usage on Europe's water resources, *Publications Office of the European Union*, Luxembourg, ISBN 978-92-79-80287-4, DOI: 10.2760/847068.

Brandt, M.J., K.M. Jonhson, A.J. Elphinston and D.D. Ratnayaka (2017) Twort's Water Supply, 7th edn., *IWA Publishing*, DOI: 0.1016/C2012-0-06331-4.

Butler, D. and F.A. Memon (2005) Water Demand Management, *IWA Publishing*, London,UK, p. 384, ISBN 1843390787.

Charalambous, B., D. Foufeas and N. Petroulias (2014) Leak detection and water loss management, *Water Utility Journal*, **8**, p.p. 25-30.

Cheung, P.B., G.V. Girol, N. Abe and M. Propato (2010) Night flow analysis and modeling for leakage estimation in a water distribution system, *Integrating Water Systems (CCWI 2010)*, *Taylor & Francis Group*, London, ISBN 978-0-415-54851-9.

Colombo, A.F., P. Lee and B.W. Karney (2009) A selective literature review of transient-based leak detection methods, *Journal of Hydro-environment Research*, **2**(4), p.p. 212–227, DOI: 10.1016/j.jher.2009.02.003.

Covas, D.I.C., A.C. Jacob and H.M. Ramos (2008) Water losses' assessment in an urban water network, *Water Practice and Technology*, **3**(3), DOI: 10.2166/wpt.2008.061.

Dallal, G.E., and L. Wilkinson (1986) An Analytic Approximation to the Distribution of Lilliefors's Test Statistic for Normality, *The American Statistician*, **40**(4), p.p. 294-296, DOI: 10.2307/2684607.

Deng, Y., M. Cardin, V. Babovic, D. Santhanakrishnan, P. Schmitter and A. Meshgi (2013) Valuing flexibilities in the design of urban water management systems, *Water Research*, **47**(20), p.p. 7162-7174, DOI: 10.1016/j.watres.2013.09.064.

Farah, E. and I. Shahrour (2017) Leakage Detection Using Smart Water System: Combination of Water Balance and Automated Minimum Night Flow, *Water Resources Management*, **31**, p.p. 4821–4833, DOI: 10.1007/s11269-017-1780-9.

Farley, M. and S. Trow (2005) Losses in Water Distribution Networks, A Practitioner’s Guide to Assessment, Monitoring and Control, *IWA Publishing*, DOI: 10.2166/9781780402642

Farley, M. (2001) *Leakage management and control: a best practice training manual*, World Health Organization, Water, Sanitation and Health Team & Water Supply and Sanitation Collaborative Council, https://apps.who.int/iris/handle/10665/66893.

Feller, W. (1968) An Introduction to Probability Theory and Its Applications: Volume I, *Wiley India Pvt. Limited*.

Ferguson, B.C., R.R. Brown, N. Frantzeskaki, F.J. de Haan and A. Deletic (2013) he enabling institutional context for integrated water management: Lessons from Melbourne, *Water Research*, **47**(20), p.p. 7300-7314, DOI: 10.1016/j.watres.2013.09.045.

Fisz, M. (1963) Probability theory and mathematical statistics. Polish Scientifique.

Gomes, R., A. Sá Marques and J. Sousa (2011) Estimation of the benefits yielded by pressure management in water distribution systems, *Urban Water Journal*, **8**(2), p.p. 65-77, DOI: 10.1080/1573062X.2010.542820.

Hamilton, S. and R. McKenzie (2014) Water Management and Water Loss, *IWA Publishing*, p 250, ISBN13: 9781780406350.

Hunaidi, O. and K. Brothers (2007) Night flow analysis of pilot DMAs in Ottawa, *Water Loss Specialist Conference, International Water Association*, Bucharest, Romania, p.p. 32-46.

IPCC, 2007: Summary for Policymakers. In: *Climate Change 2007: The Physical Science Basis. Contribution of Working Group I to the Fourth Assessment Report of the Intergovernmental Panel on Climate Change* [Solomon, S., D. Qin, M. Manning, Z. Chen, M. Marquis, K.B. Averyt, M.Tignor and H.L. Miller (eds.)]. Cambridge University Press, Cambridge, United Kingdom and New York, NY, USA.

Karadirek, I., S. Kara, G. Yilmaz, A. Muhammetoglu and H. Muhammetoglu (2012) Implementation of hydraulic modelling for water-loss reduction through pressure management, *Water Resources Management*, **26**(9), p.p. 2555–2568, DOI: 10.1007/s11269-012-0032-2.

Karathanasi, I., and C. Papageorgakopoulos (2016) Development of a Leakage Control System at the Water Supply Network of the City of Patras, *Procedia Engineering*, **162**, p.p. 553-558, DOI: 10.1016/j.proeng.2016.11.100.

Lambert, A. and A. Lalonde (2005) Using practical predictions of Economic Intervention Frequency to calculate Short-run Economic Leakage Level, with or without Pressure Management, *IWA Specialised Conference 'Leakage 2005'*, Halifax, Nova Scotia, Canada.

Lambert, A. and R. Taylor (2010) Water Loss Guidelines–Water New Zealand, ISBN 978-0-9941243-2-6.

Lambert, A., T.G. Brown, M. Takizawa and D. Weimer (1999) A Review of Performance Indicators for Real Losses from Water Supply Systems, *AQUA*, **48**(6), p.p. 227-237, DOI: 10.2166/aqua.1999.0025.

Langousis, A. and V. Kaleris (2014) Statistical framework to simulate daily rainfall series conditional on upper-air predictor variables, *Water Resour. Res.*, **50**, DOI: 10.1002/2013WR014936.

Langousis, A., A. Mamalakis, R. Deidda and M. Marrocu (2016) Assessing the relative effectiveness of statistical downscaling and distribution mapping in reproducing rainfall statistics based on climate model results, *Water Resour. Res.*, **52**, DOI: 10.1002/2015WR017556.

Lee, H., S. Chung, M. Yu, J. Koo, I. Hyun and H. Lee (2005) Applicable background minimum night flow for leakage management of small district metered areas in Korea, *Water Supply*, **5**(3-4), p.p. 181-188, DOI: 10.2166/ws.2005.0098.

Liemberger, R. and M. Farley (2004) Developing a nonrevenue water reduction strategy Part 1: Investigating and assessing water losses, *IWA WWC 2004 Conference*, Marrakech, Morocco.

Lilliefors, H. W. (1967) On the Kolmogorov-Smirnov Test for Normality with Mean and Variance Unknown, *Journal of the American Statistical Association*, **62**, p.p. 399-402, DOI: 10.2307/2283970.

Loureiro, D., R. Borba, M. Rebelo, H. Alegre, S. Coelho, D. Covas, C. Amado, A. Pacheco, A. Pina (2010) Analysis of household night-time consumption, *10th international* *conference on computing and control for the water industry, CCWI 2009, Integrating Water Systems*, Sheffield, UK.

MacDonald, G. and C. Yates (2005) DMA design and implementation, an American context, *IWA Specialized Conference Leakage*, Halifax, Nova Scotia, Canada.

Makaya, E. (2017) Predictive Leakage Estimation using the Cumulative Minimum Night Flow Approach, *American Journal of Water Resources*, **5**(1), p.p. 1-4, DOI: 10.12691/AJWR-5-1-1.

Mamalakis, A., A. Langousis, R. Deidda and M. Marrocu (2017) A parametric approach for simultaneous bias correction and high-resolution downscaling of climate model rainfall, *Water Resour. Res.*, **53**, DOI: 10.1002/2016WR019578.

Mazzolani, G., L. Berardi, D. Laucelli, R. Martino, A. Simone and O. Giustolisi (2016) A methodology to estimate leakages in water distribution networks based on inlet flow data analysis, *Procedia Engineering*, **162**, p.p. 411 – 418., DOI: 10.1016/j.proeng.2016.11.082.

Meseguer, J., J.M. Mirats-Tur, G. Cembrano, V. Puig, J. Quevedo, R. Pérez, G. Sanz and D. Ibarra (2014) A decision support system for on-line leakage localization, *Environmental Modelling & Software*, **60**, p.p. 331-345, DOI: 10.1016/j.envsoft.2014.06.025.

Morrison, J., S. Tooms and D. Rogers (2007) DMA Management Guidance Notes, *IWA Publication*, p. 100.

Muhammetoglu, A., Y. Albayrak, M. Bolbol, S. Enderoglu and H. Muhammetoglu (2020) Detection and Assessment of Post Meter Leakages in Public Places Using Smart Water Metering, *Water Resources Management*, **34**, p.p. 2989-3002, DOI: 10.1007/s11269-020-02598-1.

Papoulis, A. (1990) Probability & statistics. Vol. 2, *Prentice-Hall Englewood Cliffs*.

Parzen, E. (1960) Modern probability theory and its applications. *John Wiley & Sons, Incorporated*.

Peters, E.J. and Y. Ben-Ephraim (2012) System leakage by night flow analysis: a case study in Guyana, *Water management*, **165**(8), p.p. 451-457, DOI: 10.1680/wama.10.00112.

Petroulias, N., D. Foufeas and E. Bougoulia, (2016) Estimating Water Losses and Assessing Network Management Intervention Scenarios: The Case Study of the Water Utility of the City of Drama in Greece, *Procedia Engineering*, **162**, p.p. 559-567, DOI: 10.1016/j.proeng.2016.11.101.

Quevedo, J., R. Pérez, J. Pascual, V. Puig, G. Cembrano and A. Peralta (2012) Methodology to Detect and Isolate Water Losses in Water Hydraulic Networks: Application to Barcelona Water Network, IFAC Proceedings Volumes, **45**(20), p.p. 922-927, DOI: 10.3182/20120829-3-MX-2028.00120.

Rehan, R., M.A. Knight, A.J.A. Unger and C.T. Haas (2013) Development of a system dynamics model for financially sustainable management of municipal watermain networks, *Water Research*, **47**(20), p.p. 7184-7205, DOI: 10.1016/j.watres.2013.09.061.

Serafeim, A.V. (2018) Statistical Estimation of Water Losses in the Water Distribution Network (WDN) of the City of Patras, MSc Thesis, *Department of Civil Engineering, University of Patras*, Patra, Greece, p. 275 (in Greek).

Tabesh, M., A.H.A. Yekta and R. Burrows (2009) An integrated model to evaluate losses in water distribution systems, *Water Resources Management*, **23**(3), p.p. 477–492, DOI: 10.1007/s11269-008-9284-2.

Thornton, J., R. Sturm and G. Kunkel (2008) Water loss control, 2nd Edition, *McGraw-Hill*, NY, p. 650, DOI: 10.1036/0071499180.

Tsakiris, G. and B. Charalambous (2010) Management of Water Supply Networks, In: Hydraulic Works - Design and Management, Vol. 1: Urban Hydraulic Works, Edt. G. Tsakiris, *Symmetria*, Athens, Greece, pp. 445-482 (in Greek).

Tzanakakis, V.A., A.N. Angelakis, N.V. Paranychianakis, Y.G. Dialynas and G. Tchobanoglous (2020) Challenges and Opportunities for Sustainable Management of Water Resources in the Island of Crete, Greece, *Water*, **12**(6), 1538, DOI: 10.3390/w12061538.

UN-Habitat Lake Victoria Water and Sanitation Initiative team and National Water and Sewerage Corporation team, R. Goodwin, R. Kaggwa and A. Malebo (2012) *Utility Management Series for Small Towns, Leakage Control Manual*, **5**, UN-Habitat, ISBN: 978-92-1-132537-9.

Verde, D., E. Cima, M. Ferrante, B. Brunone and S. Meniconi (2014) The Dependence of District Minimum Night Flow on Pressure Head: The Case Study of Lenola, *Procedia Engineering*, **89**, p.p. 1224-1230, DOI: 10.1016/j.proeng.2014.11.424.

Wainstein L.A. and V.D. Zubakov (1970) Extraction of Signals from Noise, Dover Publications Inc., NY, ISBN: 0-486-62625-3.

WSAA (2011) Guidelines relating to the subject og Targeting Leakage Using Nightflow Measurements, by Wide Bay Water Corporation, Australia and Water Loss Research & Analysis Ltd, UK, *Water Services Association of Australia*.

Table Captions

Table 1: Name, total area and length of the pipeline grid of the pressure management areas (PMAs) of the city of Patras. Numbers indicate their location in Figure 1.

Table 2: Pressure set points during day ($P_{s,d}$, 06:00 am – 00:00 am) and night ($P_{s,n}$, 00:00 am – 06:00 am) hours for the low consumption period from 01 November 2018 – 28 February 2019. Q_d and Q_n denote the average flows during day and night hours, respectively, over the whole 4-month period. Station numbers are in complete correspondence with the entries in Table 1 and Figure 1.

Table 3: Statistics of minimum night flow (MNF) estimates obtained by applying Method 1 and Method 2 (values in square brackets) to different PMAs of Patras WDN; see main text for details. $\bar{Q}_{min,D^*}$ and σ_Q for Method 1, and $\bar{Q}_{lmod}$ and σ_{Qlm} for Method 2, denote, respectively the ensemble mean and standard deviation of the individual MNF estimates obtained in different days of the low consumption period from 01 November 2018 – 28 February 2019. p-values have been calculated by applying Lilliefors's test for normality to the individual MNF estimates. Bold letters indicate PMAs where the null hypothesis of normality is rejected at the 5% significance level, where equation (6) (for Method 1) or equation (10) (for Method 2) are not applicable. Station numbers are in complete correspondence with the entries in Table 1 and the PMAs illustrated in Figure 1.

Table 4: Ensemble mean m_d, standard deviation σ_d, and p-value of Lilliefors's test for normality, of the correlation length estimates d_j obtained for each day j in the low consumption period from 01 November 2018 – 28 February 2019, resulting from application of Method 1 to each pressure management area (PMA) of Patras water distribution network (WDN, see main text for details). Bold letters indicate PMAs

where the null hypothesis of normality is rejected at the 5% significance level. Station numbers are in complete correspondence with the entries in Table 1 and the PMAs illustrated in Figure 1.

Table 5: Periods and applied pressure ranges for the flow - pressure tests conducted in 43 PMAs of Patras WDN; see main text for details. Station numbers are in complete correspondence with the entries in Table 1 and the PMAs illustrated in Figure 1.

Figure Captions

Figure 1: Map indicating the locations of Patras pressure management areas (PMAs). Numbers correspond to the entries in Table 1.

Figure 2: Average flows for various window sizes D in the range from 1 min to 3 hours (i.e. 180 min) for pressure management area (PMA) "Kentro" (the largest PMA of the Municipality of Patras; see Figure 1) on 27 December, 2018 in the time frame from 00:00 am to 06:00 am; see main text for details.

Figure 3: Observed flow minima $Q^{(j)}_{min,D}$ of the time series in Figure 2 (i.e. for j set to 27 December 2018), as a function of the averaging duration D; see main text for details.

Figure 4: Ensemble mean $\bar{Q}_{min,D}$ of the observed flow minima $Q^{(j)}_{min,D}$ in different days j of the low consumption period from 01 November 2018 – 28 February 2019 in pressure management area (PMA) "Kentro", as a function of the averaging duration D.

Figure 5: Normal probability plot of the empirical CDF (circles) of the d_j estimates for pressure management area (PMA) "Kentro", obtained by calculating the correlation length of the flow time series during the night hours of each day j in the low consumption period from 01 November 2018 – 28 February 2019; see main text for details. The dashed line corresponds to a normal distribution model with mean value and variance equal to those of the d_j estimates, and the gray shaded area denotes the 95% confidence band of the theoretical quantiles.

Figure 6: Normal probability plot of the empirical CDF (circles) of the minimum average flows $Q^{(j)}_{min,D*}$ in different days j of the low consumption period from 01 November 2018 – 28 February 2019 in pressure management area (PMA) "Kentro", for size of the averaging window D^* = 120 min; see main text for details. The dashed line

corresponds to a normal distribution model with mean value and variance equal to those of the $Q^{(j)}_{min,D*}$ estimates, and the gray shaded area denotes the 95% confidence band of the theoretical quantiles.

Figure 7: Illustration of the three distinct regions characterizing the flow measurements in pressure management area (PMA) “Kentro” on 27 December 2018, within the time frame from 00:00 am to 06:00 am: a) 1-min resolution timeseries, and b) their corresponding empirical probability density function (PDF); see main text for details.

Figure 8: Normal probability plot of the empirical CDF (circles) of the lowest modal values, $Q^{(j)}_{lmod}$, of the flow time series in pressure management area (PMA) “Kentro” during the night hours of different days *j* in the low consumption period from 01 November 2018 – 28 February 2019 (a total of 119 values); see main text for details. The dashed line corresponds to a normal distribution model with mean value and variance equal to those of the $Q^{(j)}_{lmod}$ estimates, and the gray shaded area denotes the 95% confidence band of the theoretical quantiles.

Figure 9: Visual comparison of the point estimates for the average MNF, as obtained from application of Methods 1 and 2 to the 62 analyzed PMAs of Patras WDN (see also Table 3), for the 4-monthy low consumption period.

Figure 10: MNF estimates as a function of pressure, obtained from application of Method 1 to the time series resulting from the flow-pressure tests conducted in PMAs: (a) Ano_syxaina_1 (4), b) Pagona_H (64), c) Bounteni_4 (26), d) Bounteni_5 (27), e) Elekistra_1_2_3 (36), f) Elekistra_4 (37), g) Elos (38), and h) Karya_5 (49). Numbers in parentheses are in complete correspondence with the entries in Table 1 and the PMAs illustrated in Figure 1.

Table 1: Name, total area and length of the pipeline grid of the pressure management areas (PMAs) of the city of Patras. Numbers indicate their location in Figure 1.

Local Station Name	Area (m^2)	Pipeline length (m)	Local Station Name	Area (m^2)	Pipeline length (m)
(1) Amfitrionos	336585	6770	(44) Ities_lefka_H	468955	11460
(2) Ano_poli_H	327784	13540	(45) Ities_lefka_L	926148	13448
(3) Ano_poli_L	446946	25722	(46) Karya_1	39961	586
(4) Ano_syxaina_1	213127	1742	(47) Karya_2	46094	556
(5) Ano_syxaina_2	333497	2719	(48) Karya_3	10064	184
(6) Aroi_H	88173	2045	(49) Karya_5	16147	262
(7) Aroi_L	187126	6045	(50) Karya_6	90812	1283
(8) Aroi_L_a	13402	635	(51) Karya_7	163435	2085
(9) Aroi_L_b	47763	1647	(52) Karya_8	195871	2545
(10) Aroi_M_1	57182	1277	(53) Kastel_H_a	304250	8710
(11) Aroi_M_2	64818	2435	(54) Kastel_H_b	143903	2210
(12) Australias	343353	10507	(55a) Kastel_L_a	181217	7662
(13) Belbitsi_2a	130053	965	(55b) Kastel_L_b	469109	13420
(14) Belbitsi_2b	73964	869	(56) Kentro	1206867	62174
(15) Belbitsi_2c	40775	538	(57) Korydaleos	215238	4219
(16) Belbitsi_2d	107122	1487	(58) Ladonos	482742	6343
(17) Belbitsi_5_1_b	315545	2371	(59) Lyberopoulou	14654	178
(18) Biopa_H_a	313513	11646	(60) Med_Frigo	373423	2314
(19) Biopa_H_b	212784	4565	(61) Meilixou	183396	6239
(20) Biopa_M_a	251256	9316	(62) Myribili	246673	5818
(21) Biopa_M_b	172496	3150	(63) Neo_Souli	153732	1545
(22) Boud	952568	44954	(64) Pagona_H	100401	2285
(23) Bounteni_1	69432	921	(65) Pagona_L	82332	2032
(24) Bounteni_2	554971	4201	(66) Pelopos	689086	17376
(25) Bounteni_3	59156	446	(67) Periandrou	833924	21645
(26) Bounteni_4	43280	343	(68) Porfyra	106010	2327
(27) Bounteni_5	24143	266	(69) Pratsika_H	660734	32298
(28) Bounteni_6	135353	905	(70) Pratsika_L	1094830	37005
(29) Bounteni_7	145767	712	(71) Profitis_Ilias	170028	1829
(30) Bozaitika_H	93276	2353	(72) Prosfygika	801557	43246
(31) Bozaitika_L	279145	6954	(73) Psarofai	215927	6821
(32) Bozaitika_M	109192	2673	(74) Romanos	178429	1427
(33) Diagora	352514	12764	(75) Samakia_L	133305	4652
(34) Diakidi	777057	15965	(76) Stadio	1169041	20770
(35) Eftalioti	155788	1987	(77) Synora	106897	2941
(36) Elekistra_1_2_3	969550	3254	(78) Syxaina_1_2	454629	2732
(37) Elekistra_4	75143	658	(79) Syxaina_3	909210	15259
(38) Elos	523989	2315	(80) Taraboura	659413	24132
(39) Ergodynamiki	131784	851	(81) Vlatero	109617	5194
(40) Evinou	110785	1773	(82) Zarouhleika_H	736162	24639
(41) Evridiadou	318873	8863	(83) Zarouhleika_L	1161462	32693
(42) Favierou	119427	6897	(84) Zavlani	158086	4387
(43) Ities_lefka_biopa	110690	2938	(85) Panachaiki	1184264	51703

Table 2: Pressure set points during day ($P_{s,d}$, 06:00 am – 00:00 am) and night ($P_{s,n}$, 00:00 am – 06:00 am) hours for the low consumption period from 01 November 2018 – 28 February 2019. Q_d and Q_n denote the average flows during day and night hours, respectively, over the whole 4-month period. Station numbers are in complete correspondence with the entries in Table 1 and Figure 1.

Station no.	$P_{s,d}$ (atm)	Q_d (l/s)	$P_{s,n}$ (atm)	Q_n (l/s)	Station no.	$P_{s,d}$ (atm)	Q_d (l/s)	$P_{s,n}$ (atm)	Q_n (l/s)
(1)	2.69	24.7	2.30	17.8	(53)	4.00	4.50	4.00	2.79
(2)	2.61	46.4	2.25	31.8	(54)	3.75	8.23	3.00	5.86
(3)	3.60	23.4	3.00	11.5	(55a)	2.90	2.63	2.36	1.66
(4)	2.73	0.73	2.73	0.27	(55b)	2.58	6.85	2.46	5.04
(7)	3.00	5.85	2.70	2.48	(56)	3.54	110	3.06	76.6
(9)	3.60	1.54	3.60	0.61	(57)	3.30	0.53	2.70	0.29
(10)	3.30	6.58	2.82	2.73	(58)	3.50	4.50	3.12	2.23
(12)	3.93	4.60	3.42	1.94	(59)	2.50	0.36	2.40	0.22
(22)	2.30	49.3	2.30	29.6	(60)	2.60	1.06	2.60	0.79
(24)	3.90	2.67	3.67	1.31	(61)	4.47	7.75	4.00	4.38
(25)	3.50	0.58	3.50	0.33	(62)	2.10	3.26	2.10	2.18
(26)	3.36	0.24	3.36	0.17	(63)	2.70	2.83	2.10	2.43
(27)	3.00	0.12	2.50	0.08	(64)	2.40	2.48	2.11	1.10
(31)	2.69	4.07	2.30	2.02	(65)	3.20	1.67	2.70	0.75
(33)	4.70	13.3	4.30	7.09	(66)	3.29	14.9	2.70	9.48
(34)	1.80	18.3	1.50	16.2	(67)	3.58	25.5	3.34	18.6
(35)	3.30	0.95	2.63	0.45	(68)	3.30	0.71	3.00	0.34
(36)	3.00	1.66	3.00	1.45	(69)	3.30	46.4	3.01	32.5
(37)	2.00	0.16	2.00	0.13	(71)	3.50	0.16	3.50	0.08
(38)	1.80	0.44	1.80	0.35	(72)	3.96	45.4	3.39	29.4
(41)	3.90	11.9	3.78	10.7	(73)	2.00	3.99	2.00	3.74
(42)	3.88	9.72	3.65	6.15	(74)	5.10	1.56	4.30	0.95
(43)	2.16	2.97	1.50	2.45	(75)	3.30	2.48	2.70	1.93
(44)	3.29	7.20	2.40	4.60	(76)	3.56	31.3	3.30	24.7
(45)	3.29	7.24	2.10	3.94	(77)	4.10	7.39	3.57	5.18
(47)	7.11	2.02	6.92	1.97	(78)	3.00	4.04	3.00	3.79
(48)	4.50	0.54	4.50	0.27	(79)	2.90	4.02	2.40	3.71
(49)	2.40	0.61	2.40	0.29	(81)	2.60	5.18	2.10	3.13
(50)	3.30	0.29	3.30	0.23	(82)	4.00	14.8	3.00	7.03
(51)	3.00	5.42	3.00	4.07	(83)	4.20	18.9	3.33	9.20
(52)	2.70	4.22	2.10	3.47	(84)	4.50	3.55	4.50	1.71

Table 3: Statistics of minimum night flow (MNF) estimates obtained by applying Method 1 and Method 2 (values in square brackets) to different PMAs of Patras WDN; see main text for details. $\bar{Q}_{min,D*}$ and σ_Q for Method 1, and $\bar{Q}_{lmod}$ and σ_{Qlm} for Method 2, denote, respectively the ensemble mean and standard deviation of the individual MNF estimates obtained in different days of the low consumption period from 01 November 2018 – 28 February 2019. *p*-values have been calculated by applying Lilliefors's test for normality to the individual MNF estimates. Bold letters indicate PMAs where the null hypothesis of normality is rejected at the 5% significance level, where equation (6) (for Method 1) or equation (10) (for Method 2) are not applicable. Station numbers are in complete correspondence with the entries in Table 1 and the PMAs illustrated in Figure 1.

Station no.	$\bar{Q}_{min,D*}$ or [$\bar{Q}_{lmod}$] (l/s)	σ_Q or [σ_{Qlm}] (l/s)	*p*-value	95% confidence intervals (l/s)	
				lower limit	upper limit
(1)	17.13 [17.47]	0.89 [0.88]	0.078 [0.193]	16.97 [17.31]	17.29 [17.63]
(2)	26.45 [27.05]	1.14 [1.09]	0.158 [0.404]	26.25 [26.85]	26.65 [27.25]
(3)	9.790 [10.07]	0.60 [0.65]	0.523 [0.435]	9.682 [9.953]	9.898 [10.19]
(4)	0.140 [0.150]	0.02 [0.02]	0.526 [0.354]	0.136 [0.146]	0.144 [0.154]
(7)	1.840 [1.900]	0.06 [0.03]	0.237 [0.189]	1.829 [1.895]	1.851 [1.905]
(9)	0.390 [0.410]	0.03 [0.03]	0.518 [0.174]	0.385 [0.405]	0.395 [0.415]
(10)	2.080 [2.110]	0.17 [0.10]	0.095 [0.100]	2.049 [2.092]	2.111 [2.128]
(12)	1.170 [1.220]	0.06 [0.06]	0.099 [0.932]	1.159 [1.209]	1.181 [1.231]
(22)	26.31 [26.68]	0.35 [0.55]	0.051 [0.511]	26.25 [26.58]	26.37 [26.78]
(24)	0.840 [0.860]	0.11 [0.17]	0.162 [0.211]	0.820 [0.829]	0.860 [0.891]
(25)	0.210 [0.220]	0.02 [0.02]	0.277 [0.054]	0.206 [0.216]	0.214 [0.224]
(26)	0.130 [0.140]	0.02 [0.03]	**0.001 [0.024]**	-	-
(27)	0.070 [0.070]	0.03 [0.02]	**0.001 [0.043]**	-	-
(31)	1.790 [1.830]	0.12 [0.14]	0.059 [0.443]	1.768 [1.805]	1.812 [1.855]
(33)	4.300 [4.390]	0.02 [0.02]	0.237 [0.294]	4.296 [4.386]	4.304 [4.394]
(34)	9.160 [9.460]	0.11 [0.12]	0.187 [0.071]	9.140 [9.438]	9.180 [0.482]
(35)	0.350 [0.370]	0.02 [0.01]	0.093 [0.864]	0.346 [0.368]	0.354 [0.372]
(36)	1.330 [1.380]	0.50 [0.46]	**0.001 [0.001]**	-	-
(37)	0.110 [0.120]	0.06 [0.07]	**0.001 [0.001]**	-	-
(38)	0.330 [0.340]	0.05 [0.05]	**0.001 [0.001]**	-	-
(41)	10.30 [10.63]	0.21 [0.10]	0.145 [0.472]	10.26 [10.61]	10.34 [10.65]
(42)	5.210 [5.270]	0.21 [0.52]	0.366 [0.070]	5.172 [5.177]	5.248 [5.363]
(43)	2.360 [2.410]	0.05 [0.05]	0.070 [0.165]	2.351 [2.401]	2.369 [2.419]
(44)	4.480 [4.400]	0.80 [0.76]	0.685 [0.411]	4.336 [4.263]	4.624 [4.537]
(45)	3.580 [3.670]	0.34 [0.19]	0.514 [0.391]	3.519 [3.636]	3.641 [3.704]
(47)	1.840 [1.920]	0.05 [0.02]	0.547 [0.103]	1.831 [1.916]	1.849 [1.924]
(48)	0.220 [0.230]	0.01 [0.02]	0.273 [0.495]	0.218 [0.226]	0.222 [0.234]

(49)	0.210 [0.220]	0.08 [0.08]	**0.001 [0.001]**	-	-
(50)	0.210 [0.220]	0.08 [0.08]	0.171 [0.155]	0.196 [0.206]	0.224 [0.234]
(51)	3.080 [3.170]	0.02 [0.02]	0.241 [0.163]	3.076 [3.166]	3.084 [3.174]
(52)	3.020 [3.060]	0.05 [0.04]	0.319 [0.440]	3.011 [3.053]	3.029 [3.067]
(53)	2.410 [2.530]	0.28 [0.50]	0.324 [0.183]	2.360 [2.440]	2.460 [2.620]
(54)	5.410 [5.500]	0.19 [0.20]	0.266 [0.510]	5.376 [5.464]	5.444 [5.536]
(55a)	1.500 [1.570]	0.10 [0.13]	0.269 [0.858]	1.482 [1.547]	1.518 [1.593]
(55b)	4.630 [4.740]	0.17 [0.20]	0.368 [0.439]	4.599 [4.704]	4.661 [4.776]
(56)	69.40 [69.85]	4.37 [3.91]	0.799 [0.057]	68.61 [69.15]	70.19 [70.55]
(57)	0.230 [0.240]	0.03 [0.02]	0.510 [0.102]	0.225 [0.236]	0.235 [0.244]
(58)	1.470 [1.500]	0.04 [0.03]	0.455 [0.237]	1.463 [1.494]	1.477 [1.506]
(59)	0.150 [0.160]	0.02 [0.01]	0.102 [0.170]	0.146 [0.158]	0.154 [0.162]
(60)	0.640 [0.670]	0.03 [0.04]	0.456 [0.585]	0.635 [0.663]	0.645 [0.677]
(61)	2.670 [2.740]	0.26 [0.24]	0.198 [0.170]	2.623 [2.697]	2.717 [2.783]
(62)	1.810 [1.920]	0.12 [0.21]	0.843 [0.158]	1.788 [1.882]	1.832 [1.958]
(63)	2.200 [2.260]	0.01 [0.01]	0.176 [0.175]	2.198 [2.258]	2.202 [2.262]
(64)	0.820 [0.860]	0.04 [0.06]	0.512 [0.729]	0.813 [0.849]	0.827 [0.871]
(65)	0.570 [0.600]	0.03 [0.05]	0.325 [0.255]	0.565 [0.591]	0.575 [0.609]
(66)	8.720 [8.900]	0.54 [0.37]	0.201 [0.051]	8.623 [8.834]	8.817 [8.966]
(67)	17.31 [17.46]	0.97 [0.64]	0.550 [0.189]	17.14 [17.35]	17.48 [17.57]
(68)	0.120 [0.130]	0.01 [0.01]	0.265 [0.291]	0.118 [0.128]	0.122 [0.132]
(69)	30.86 [31.00]	0.70 [0.70]	0.056 [0.056]	30.73 [30.87]	30.99 [31.13]
(71)	0.040 [0.040]	0.01 [0.01]	0.257 [0.875]	0.038 [0.038]	0.042 [0.042]
(72)	27.56 [27.80]	1.40 [1.27]	0.786 [0.895]	27.31 [27.57]	27.81 [28.03]
(73)	2.770 [2.900]	0.12 [0.14]	0.182 [0.164]	2.748 [2.875]	2.792 [2.925]
(74)	0.580 [0.600]	0.03 [0.03]	0.622 [0.636]	0.575 [0.595]	0.585 [0.605]
(75)	1.740 [1.770]	0.03 [0.03]	0.962 [0.389]	1.735 [1.765]	1.745 [1.775]
(76)	23.95 [24.35]	0.29 [0.61]	0.061 [0.176]	23.90 [24.24]	24.00 [24.46]
(77)	5.010 [5.090]	0.10 [0.10]	0.207 [0.840]	4.992 [5.072]	5.028 [5.108]
(78)	2.820 [3.010]	0.14 [0.12]	0.200 [0.055]	2.795 [2.988]	2.845 [3.032]
(79)	2.790 [2.960]	0.09 [0.11]	0.495 [0.366]	2.773 [2.939]	2.807 [2.981]
(81)	2.180 [2.250]	0.18 [0.28]	0.151 [0.065]	2.148 [2.200]	2.212 [2.300]
(82)	6.080 [6.400]	0.80 [0.54]	0.685 [0.460]	5.936 [6.303]	6.224 [6.497]
(83)	8.230 [8.320]	0.34 [0.32]	0.514 [0.477]	8.169 [8.263]	8.291 [8.377]
(84)	1.400 [1.460]	0.11 [0.10]	0.513 [0.510]	1.380 [1.442]	1.420 [1.478]

Table 4: Ensemble mean m_d, standard deviation σ_d, and p-value of Lilliefors's test for normality, of the correlation length estimates d_j obtained for each day j in the low consumption period from 01 November 2018 – 28 February 2019, resulting from application of Method 1 to each pressure management area (PMA) of Patras water distribution network (WDN, see main text for details). Bold letters indicate PMAs where the null hypothesis of normality is rejected at the 5% significance level. Station numbers are in complete correspondence with the entries in Table 1 and the PMAs illustrated in Figure 1.

Station no.	m_d (min)	σ_d (min)	p-value	Station no.	m_d (min)	σ_d (min)	p-value
(1)	104.5	9.66	0.160	(53)	64.15	13.8	0.410
(2)	119.2	5.25	0.054	(54)	98.86	20.8	0.269
(3)	114.6	5.28	0.107	(55a)	54.37	16.4	0.051
(4)	78.07	23.5	0.500	(55b)	101.9	17.1	0.184
(7)	116.1	10.7	0.054	(56)	119.3	5.82	0.409
(9)	105.2	21.4	0.382	(57)	102.3	18.2	0.367
(10)	115.5	9.92	0.056	(58)	109.8	9.89	0.390
(12)	114.0	13.5	0.748	(59)	74.98	27.3	0.062
(22)	112.0	5.38	0.057	(60)	96.99	16.2	0.460
(24)	89.81	16.7	0.473	(61)	109.0	11.4	0.161
(25)	63.51	27.2	0.557	(62)	66.25	8.82	0.101
(26)	23.52	12.1	**0.045**	(63)	8.360	0.94	0.258
(27)	17.77	19.1	**0.001**	(64)	108.4	5.14	0.153
(31)	120.0	12.0	0.067	(65)	109.7	14.8	0.389
(33)	114.0	8.30	0.059	(66)	105.8	11.2	0.634
(34)	109.2	12.1	0.237	(67)	59.57	0.27	0.942
(35)	94.98	21.0	0.377	(68)	40.57	17.5	0.050
(36)	67.31	22.3	0.073	(69)	110.0	9.04	0.415
(37)	17.84	16.4	**0.001**	(71)	82.10	36.0	0.772
(38)	32.38	28.9	**0.001**	(72)	108.7	10.9	0.788
(41)	102.4	16.8	0.081	(73)	40.31	8.99	0.285
(42)	118.1	6.30	0.376	(74)	63.92	28.7	0.055
(43)	19.39	14.6	0.050	(75)	83.26	41.3	0.050
(44)	101.8	12.7	0.428	(76)	105.7	16.5	0.242
(45)	105.1	10.7	0.347	(77)	104.5	9.66	0.161
(47)	34.57	30.2	0.174	(78)	40.17	8.75	0.329
(48)	6.760	4.05	0.058	(79)	39.00	10.4	0.500
(49)	8.830	10.1	**0.001**	(81)	118.7	3.64	0.186
(50)	75.54	22.6	0.055	(82)	101.4	9.96	0.855
(51)	59.61	24.1	0.050	(83)	102.6	9.96	0.853
(52)	63.41	15.0	0.510	(84)	103.5	10.6	0.375

Table 5: Periods and applied pressure ranges for the flow - pressure tests conducted in 43 PMAs of Patras WDN; see main text for details. Station numbers are in complete correspondence with the entries in Table 1 and the PMAs illustrated in Figure 1.

Station no.	1st Period		2nd Period		3rd Period		Pressure (bar)		
	Start	End	Start	End	Start	End	1st	2nd	3rd
(1)	8-Dec	15-Dec	16-Dec	26-Dec	27-Dec	5-Jan	3.70	2.50	2.00
(2)	14-Nov	18-Nov	19-Nov	5-Dec	6-Dec	16-Dec	3.40	2.70	2.00
(3)	14-Nov	18-Nov	19-Nov	1-Dec	2-Dec	7-Dec	4.20	3.50	2.90
(4)	7-Jan	13-Jan	14-Jan	20-Jan	21-Jan	13-Feb	3.70	2.80	2.30
(5)	27-Dec	5-Jan	6-Jan	15-Jan	16-Jan	15-Feb	2.00	1.60	1.20
(7)	6-Dec	15-Dec	16-Dec	26-Dec	27-Dec	5-Jan	4.50	3.30	2.50
(9)	14-Nov	18-Nov	19-Nov	5-Dec	6-Dec	10-Dec	4.50	3.60	3.00
(10)	6-Dec	15-Dec	16-Dec	25-Dec	26-Dec	20-Jan	4.00	2.80	2.50
(12)	7-Dec	15-Dec	16-Dec	25-Dec	26-Dec	5-Jan	4.30	3.40	3.00
(23)	14-Nov	18-Nov	20-Nov	1-Dec	2-Dec	10-Dec	4.00	3.00	2.50
(24)	14-Nov	18-Nov	19-Nov	1-Dec	2-Dec	10-Dec	3.70	2.70	1.90
(25)	18-Nov	22-Nov	23-Nov	27-Nov	28-Nov	2-Dec	4.20	3.30	2.50
(26)	24-Nov	30-Nov	1-Dec	9-Dec	10-Dec	16-Dec	4.00	3.30	2.80
(27)	14-Nov	18-Nov	19-Nov	26-Nov	27-Nov	2-Dec	4.50	3.00	2.00
(31)	15-Nov	20-Nov	21-Nov	25-Nov	26-Nov	30-Nov	3.20	2.50	2.00
(33)	16-Dec	25-Dec	26-Dec	5-Jan	6-Jan	11-Jan	5.20	4.50	4.00
(34)	14-Nov	18-Nov	19-Nov	1-Dec	2-Dec	5-Jan	3.00	2.50	2.00
(36)	8-Dec	15-Dec	16-Dec	22-Dec	23-Dec	29-Dec	4.00	3.30	2.70
(37)	8-Dec	16-Dec	17-Dec	22-Dec	23-Dec	30-Dec	3.00	2.10	1.40
(38)	10-Dec	15-Dec	16-Dec	21-Dec	22-Dec	27-Dec	3.00	1.90	1.50
(41)	9-Jan	19-Jan	20-Jan	26-Jan	27-Jan	5-Feb	5.00	3.80	3.00
(42)	6-Dec	15-Dec	16-Dec	8-Jan	10-Jan	14-Jan	4.00	3.00	2.00
(43)	8-Dec	15-Dec	16-Dec	25-Dec	26-Dec	21-Jan	3.00	2.50	1.60
(44)	14-Nov	19-Nov	20-Nov	7-Dec	8-Dec	12-Dec	3.50	2.70	2.00
(45)	6-Feb	16-Feb	17-Feb	8-Mar	9-Mar	14-Mar	4.00	3.40	2.30
(47)	6-Feb	16-Feb	17-Feb	8-Mar	9-Mar	14-Mar	3.50	2.50	1.70
(48)	6-Dec	15-Dec	16-Dec	25-Dec	26-Dec	5-Feb	4.50	3.70	3.00
(49)	8-Dec	15-Dec	16-Dec	25-Dec	26-Dec	2-Feb	4.10	3.30	2.50
(50)	14-Dec	25-Dec	26-Dec	26-Jan	27-Jan	5-Feb	4.00	3.20	2.00
(52)	8-Dec	15-Dec	16-Dec	25-Dec	26-Dec	5-Feb	4.20	3.20	2.20
(53)	6-Dec	15-Dec	16-Dec	25-Dec	26-Dec	16-Feb	5.00	4.00	3.00
(55a)	6-Dec	25-Dec	26-Dec	16-Feb	17-Feb	29-Feb	3.70	2.40	2.00
(55b)	6-Dec	15-Dec	16-Dec	25-Dec	26-Dec	5-Feb	3.20	2.50	2.00
(56)	6-Dec	10-Dec	11-Dec	8-Jan	9-Jan	16-Feb	4.00	3.50	2.90
(57)	6-Dec	15-Dec	16-Dec	25-Dec	6-Jan	21-Feb	4.00	2.85	2.00
(60)	28-Jan	5-Feb	6-Feb	16-Feb	17-Feb	27-Feb	3.80	2.80	2.00
(61)	22-Jan	26-Jan	27-Jan	16-Feb	17-Feb	27-Feb	5.00	4.15	3.50

(64)	20-Jan	26-Jan	27-Jan	16-Feb	17-Feb	21-Feb	3.00	2.10	1.50
(78)	10-Dec	15-Dec	16-Dec	25-Dec	6-Jan	19-Jan	4.00	2.90	2.00
(79)	10-Dec	15-Dec	16-Dec	25-Dec	6-Jan	19-Jan	3.50	2.60	2.00
(82)	16-Feb	21-Feb	22-Feb	8-Mar	9-Mar	15-Mar	4.50	3.80	3.10
(83)	9-Jan	13-Jan	14-Jan	19-Jan	20-Jan	25-Jan	5.00	4.50	3.40
(84)	10-Dec	15-Dec	16-Dec	25-Dec	26-Dec	5-Jan	5.50	4.80	4.00

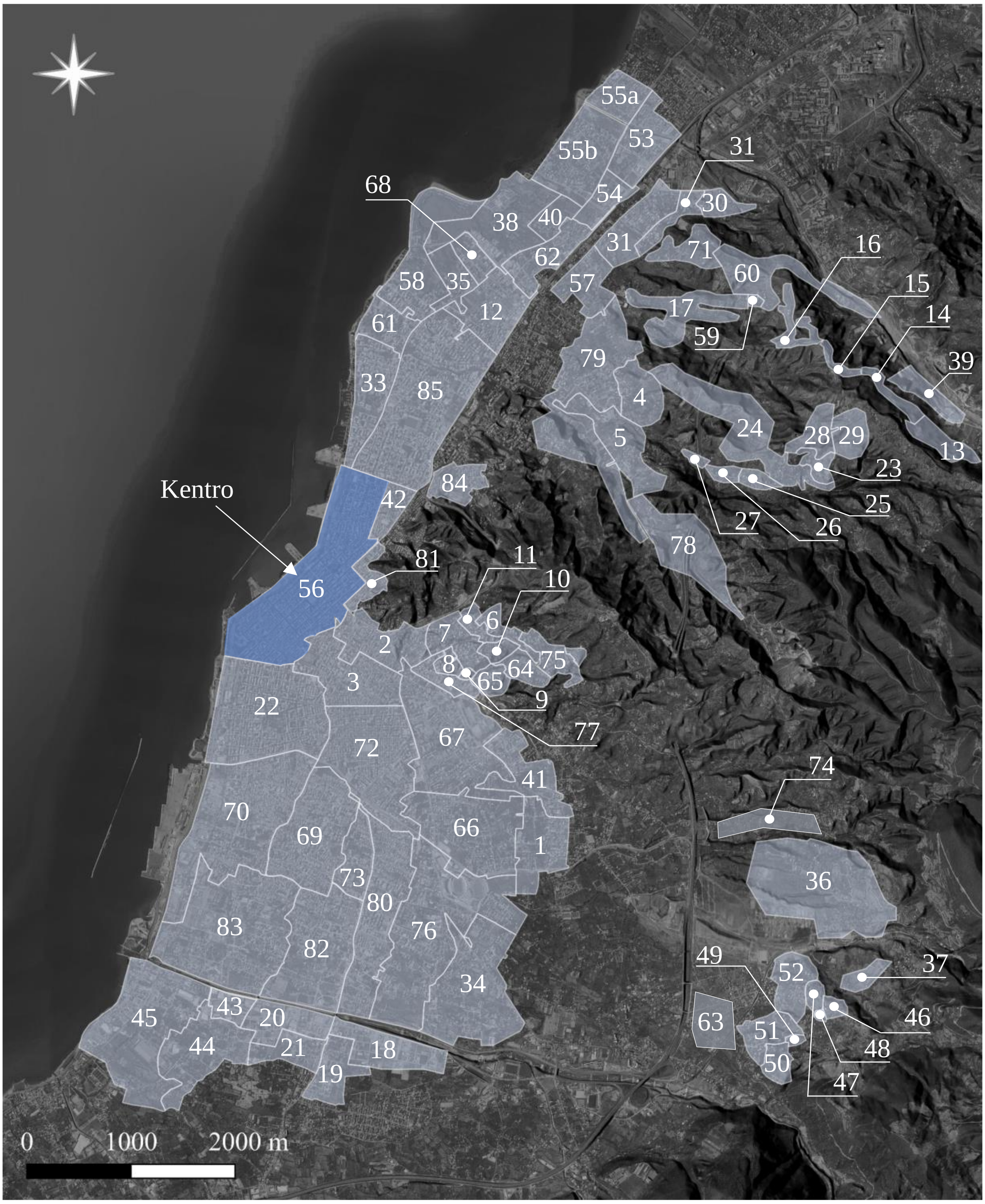

Figure 1: Map indicating the locations of Patras pressure management areas (PMAs). Numbers correspond to the entries in Table 1.

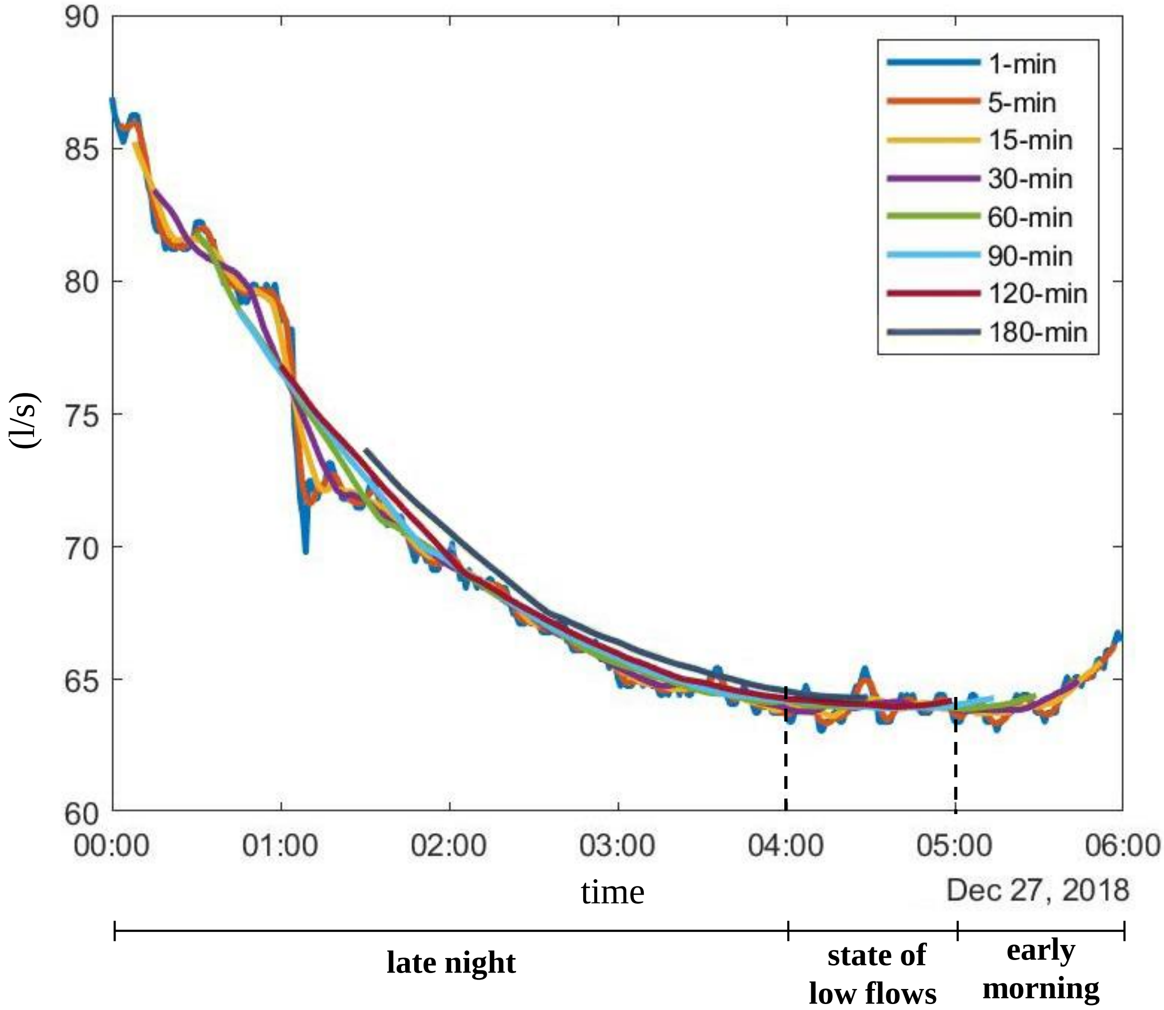

Figure 2: Average flows for various window sizes *D* in the range from 1 min to 3 hours (i.e. 180 min) for pressure management area (PMA) "Kentro" (the largest PMA of the Municipality of Patras; see Figure 1) on 27 December, 2018 in the time frame from 00:00 am to 06:00 am; see main text for details.

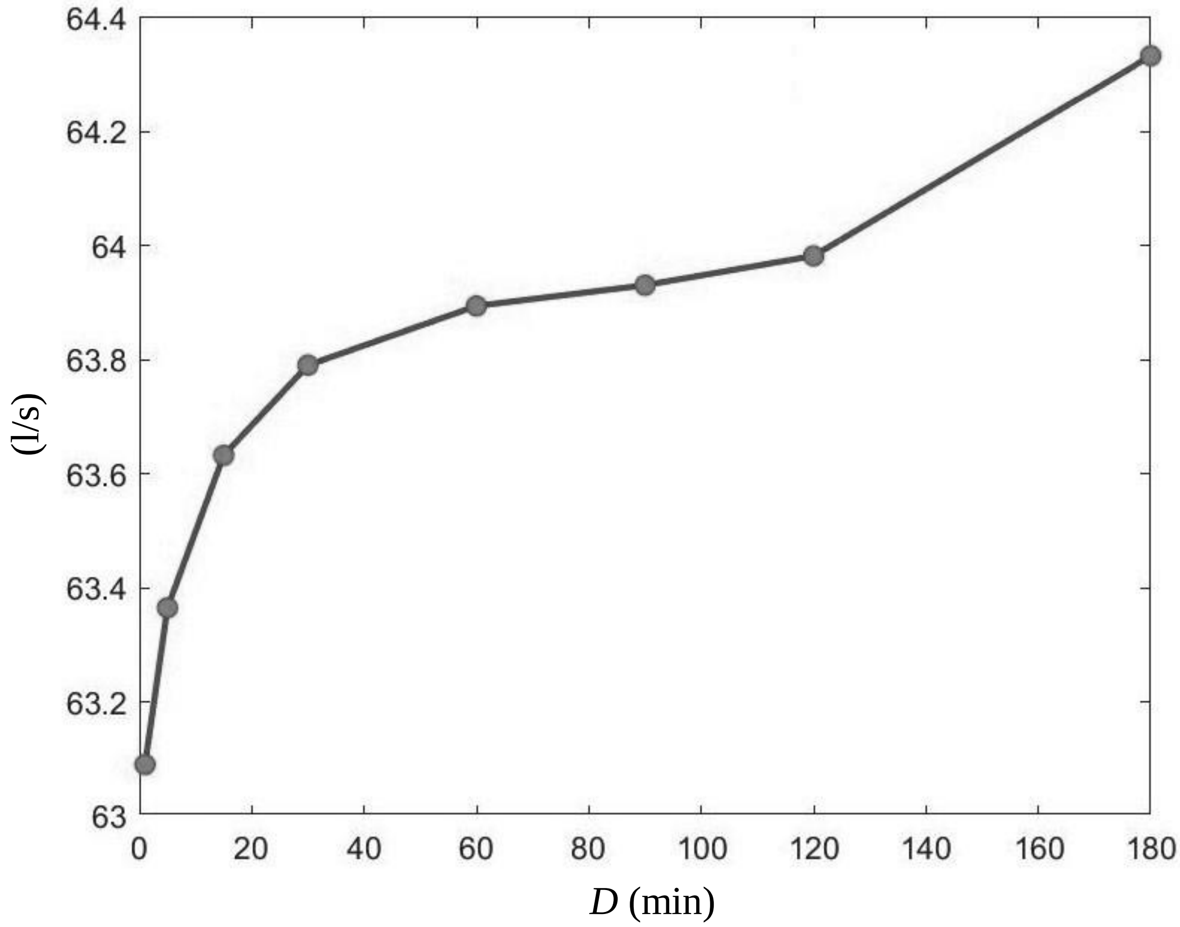

Figure 3: Observed flow minima $Q^{(j)}_{min,D}$ of the time series in Figure 2 (i.e. for j set to 27 December 2018), as a function of the averaging duration D; see main text for details.

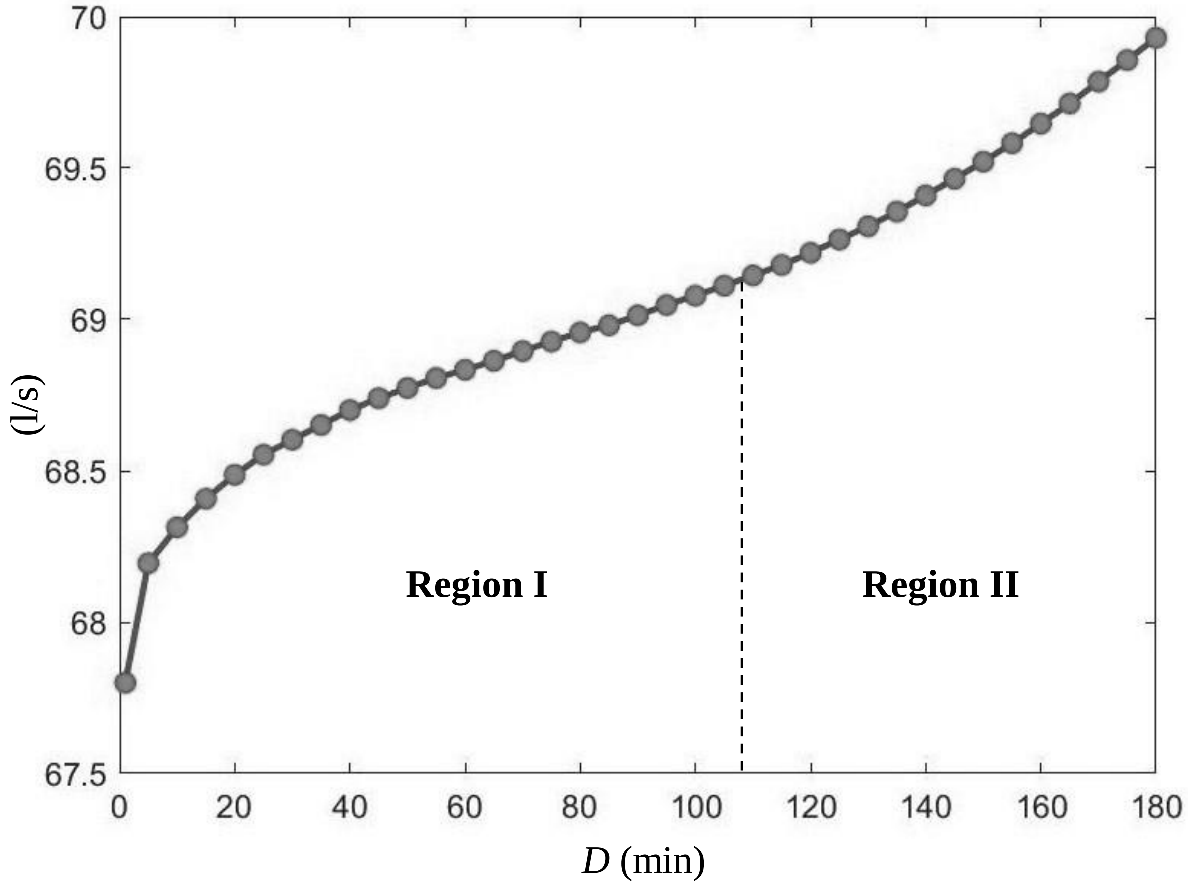

Figure 4: Ensemble mean $\bar{Q}_{min,D}$ of the observed flow minima $Q^{(j)}_{min,D}$ in different days j of the low consumption period from 01 November 2018 – 28 February 2019 in pressure management area (PMA) “Kentro”, as a function of the averaging duration D.

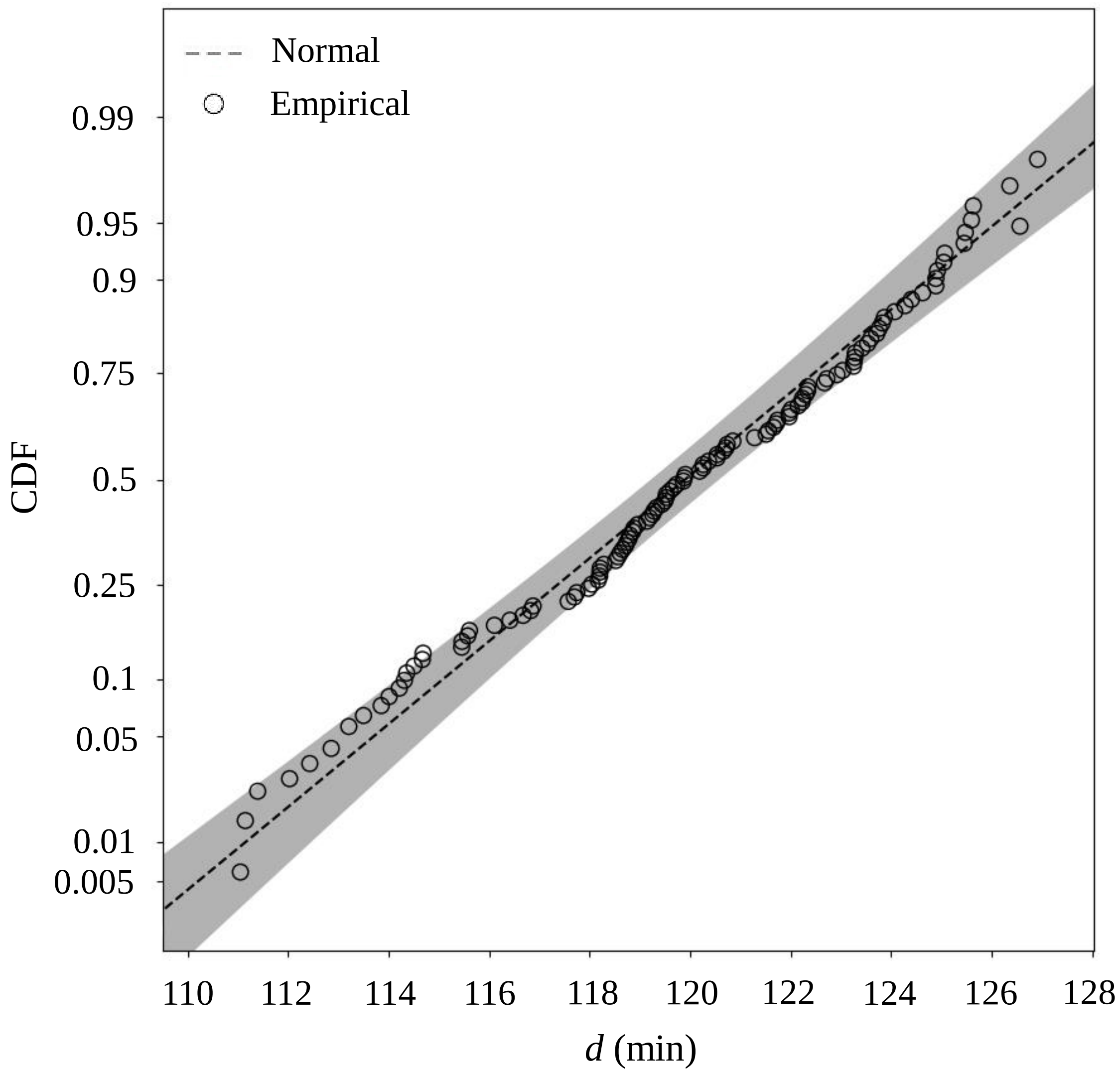

Figure 5: Normal probability plot of the empirical CDF (circles) of the d_j estimates for pressure management area (PMA) “Kentro”, obtained by calculating the correlation length of the flow time series during the night hours of each day j in the low consumption period from 01 November 2018 – 28 February 2019; see main text for details. The dashed line corresponds to a normal distribution model with mean value and variance equal to those of the d_j estimates, and the gray shaded area denotes the 95% confidence band of the theoretical quantiles.

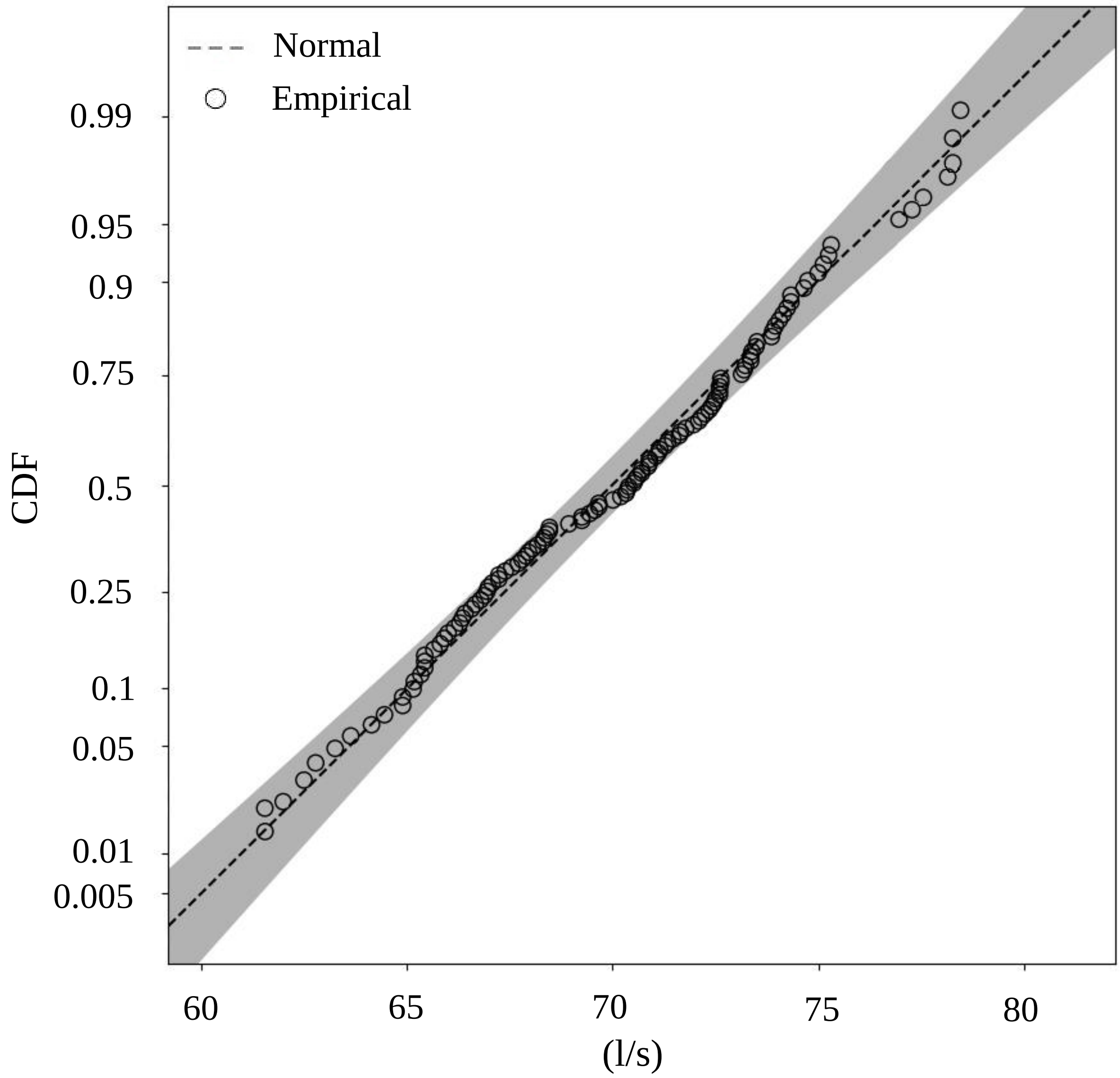

Figure 6: Normal probability plot of the empirical CDF (circles) of the minimum average flows $Q^{(j)}_{min,D^*}$ in different days j of the low consumption period from 01 November 2018 – 28 February 2019 in pressure management area (PMA) "Kentro", for size of the averaging window D^* = 120 min; see main text for details. The dashed line corresponds to a normal distribution model with mean value and variance equal to those of the $Q^{(j)}_{min,D^*}$ estimates, and the gray shaded area denotes the 95% confidence band of the theoretical quantiles.

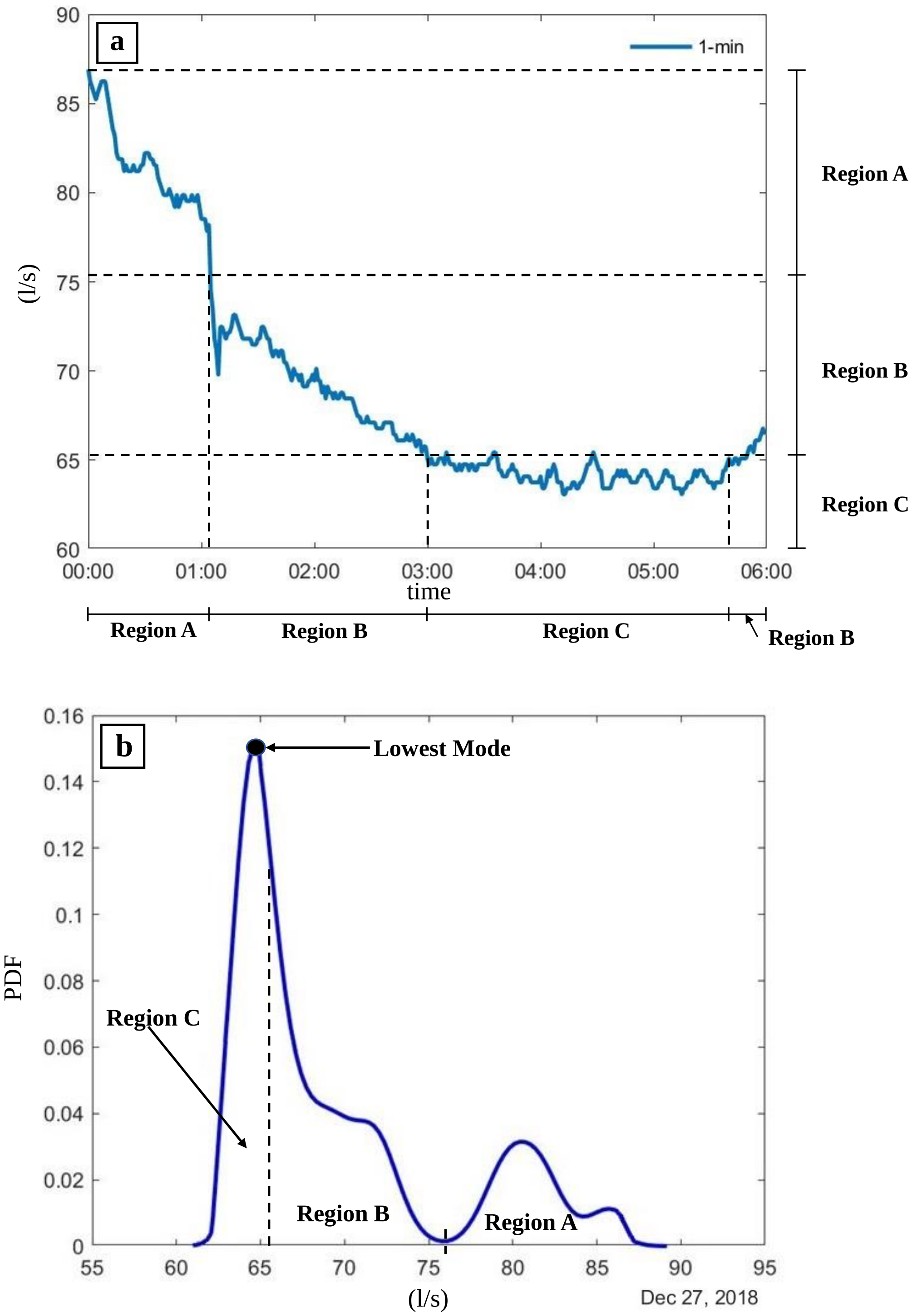

Figure 7: Illustration of the three distinct regions characterizing the flow measurements in pressure management area (PMA) “Kentro” on 27 December 2018, within the time frame from 00:00 am to 06:00 am: a) 1-min resolution timeseries, and b) their corresponding empirical probability density function (PDF); see main text for details.

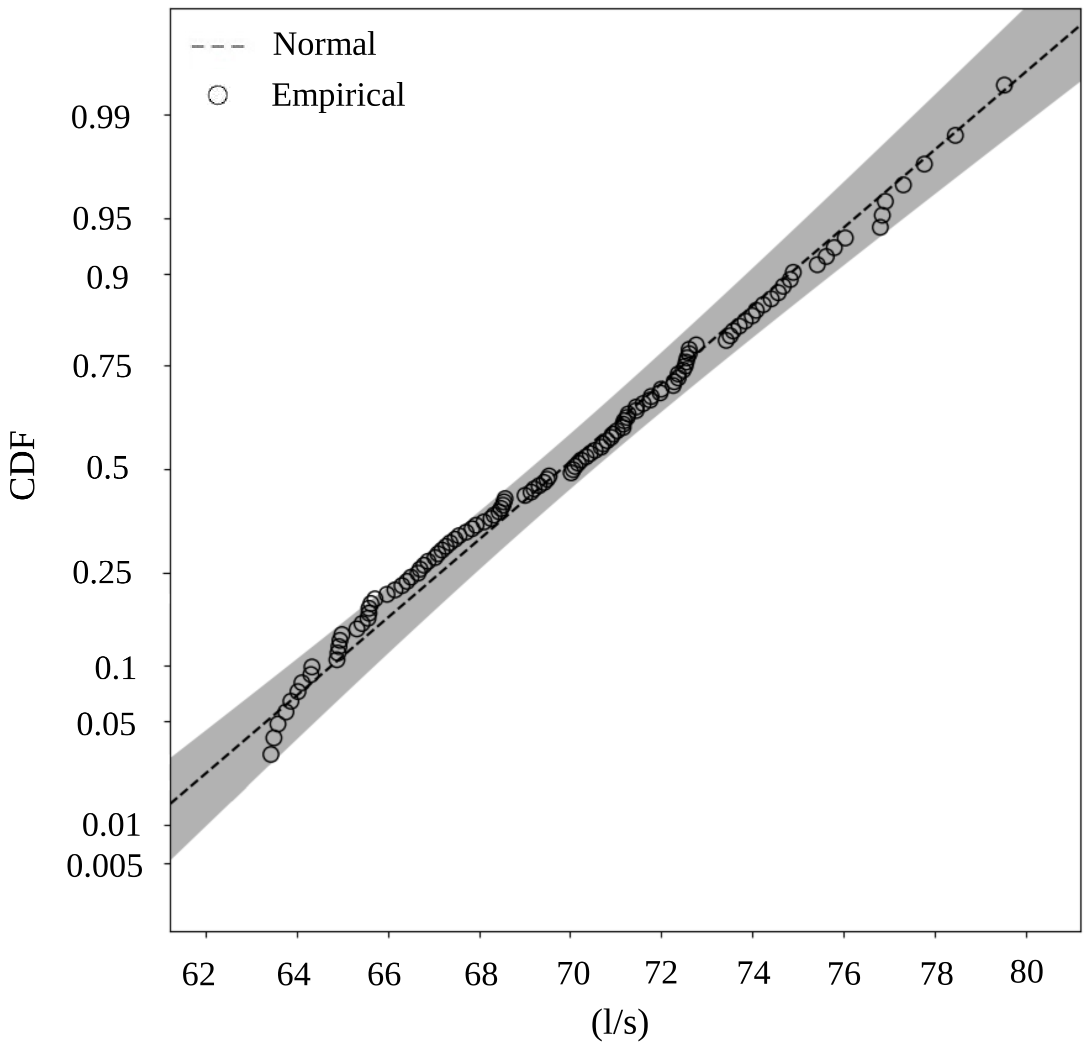

Figure 8: Normal probability plot of the empirical CDF (circles) of the lowest modal values, $Q_{lmod}^{(j)}$, of the flow time series in pressure management area (PMA) “Kentro” during the night hours of different days j in the low consumption period from 01 November 2018 – 28 February 2019 (a total of 119 values); see main text for details. The dashed line corresponds to a normal distribution model with mean value and variance equal to those of the $Q_{lmod}^{(j)}$ estimates, and the gray shaded area denotes the 95% confidence band of the theoretical quantiles.

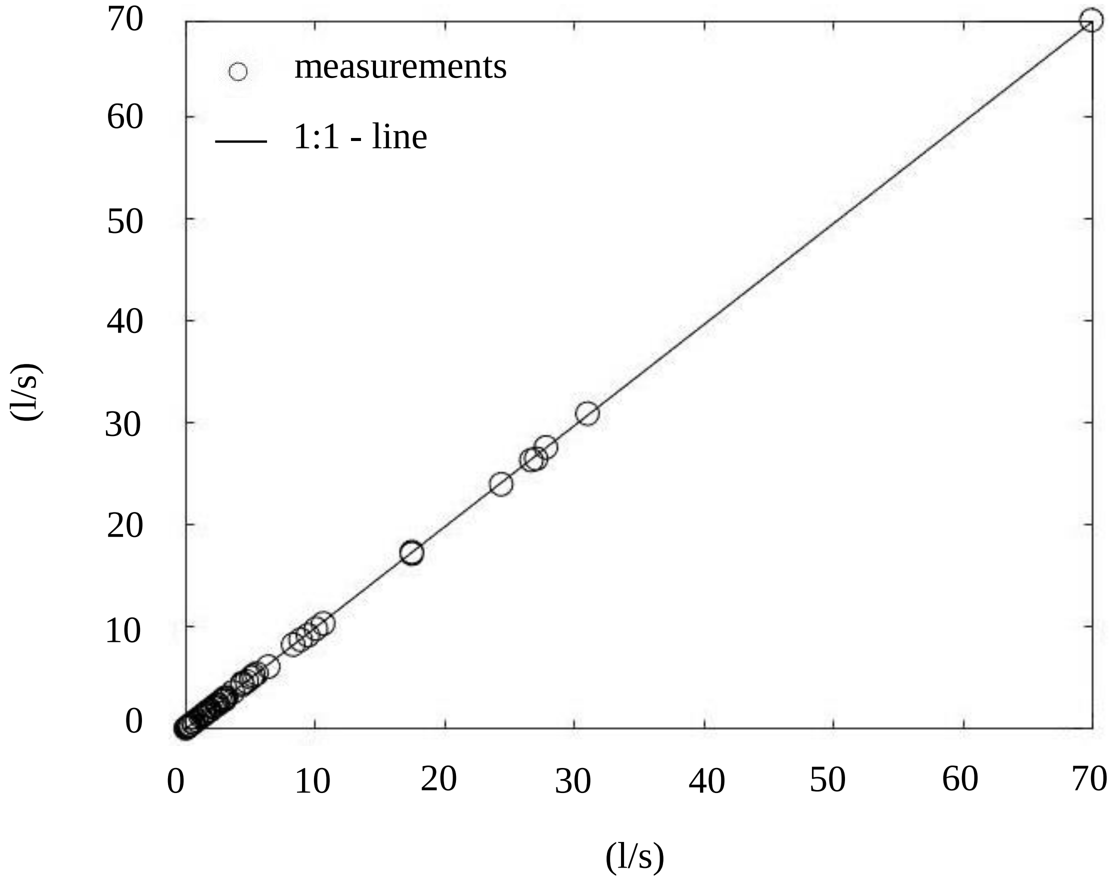

Figure 9: Visual comparison of the point estimates for the average MNF, as obtained from application of Methods 1 and 2 to the 62 analyzed PMAs of Patras WDN (see also Table 3), for the 4-monthy low consumption period.

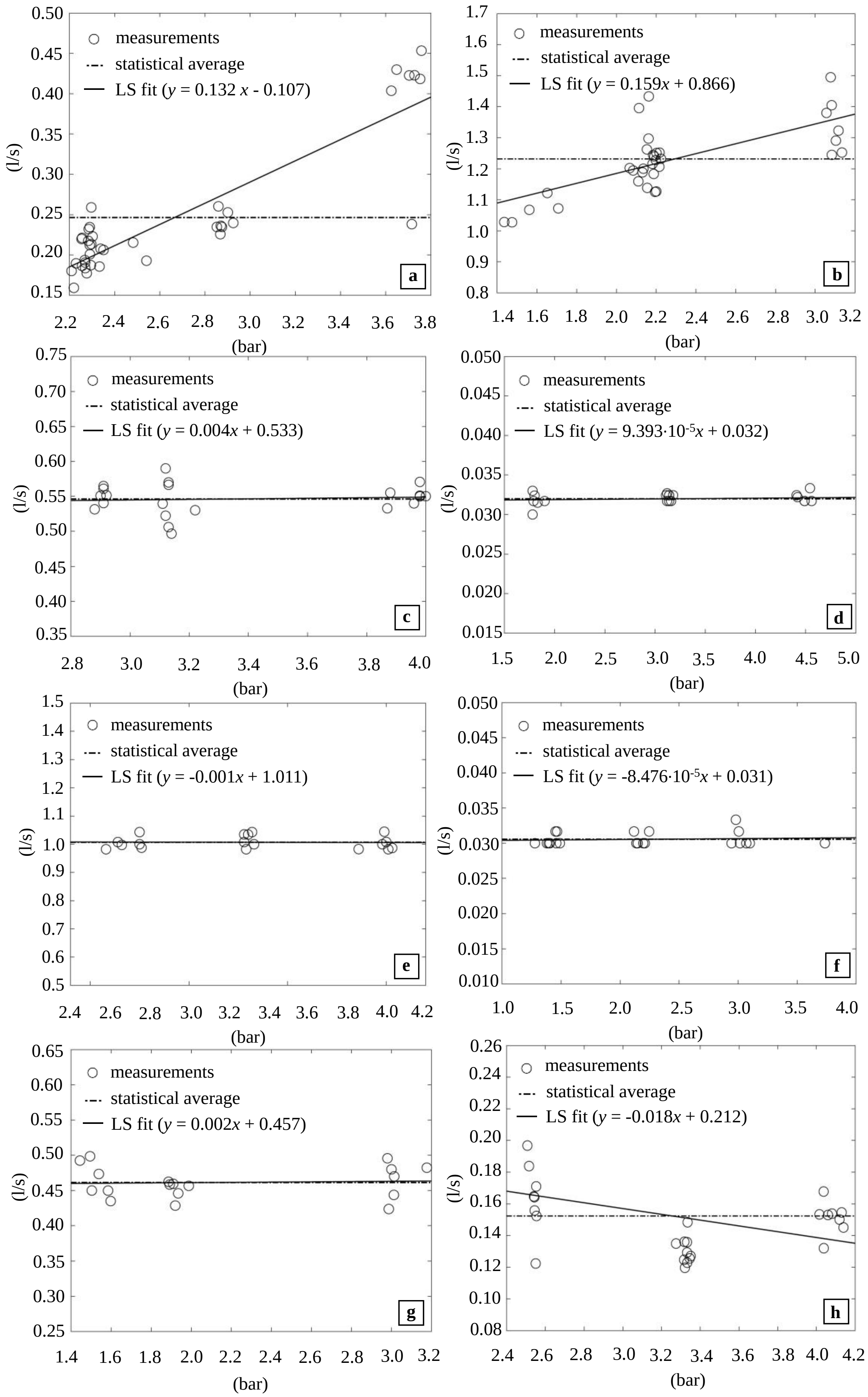
measurements
statistical average
LS fit (y = 0.132 x - 0.107)
(l/s)
(bar)
a
LS fit (y = 0.159x + 0.866)
b
LS fit (y = 0.004x + 0.533)
c
LS fit (y = 9.393·10-5x + 0.032)
d
LS fit (y = -0.001x + 1.011)
e
LS fit (y = -8.476·10-5x + 0.031)
f
LS fit (y = 0.002x + 0.457)
g
LS fit (y = -0.018x + 0.212)
h

Figure 10: MNF estimates as a function of pressure, obtained from application of Method 1 to the time series resulting from the flow-pressure tests conducted in PMAs: (a) Ano_syxaina_1 (4), b) Pagona_H (64), c) Bounteni_4 (26), d) Bounteni_5 (27), e) Elekistra_1_2_3 (36), f) Elekistra_4 (37), g) Elos (38), and h) Karya_5 (49). Numbers in parentheses are in complete correspondence with the entries in Table 1 and the PMAs illustrated in Figure 1.